REVIEW OF RF POWER SOURCES FOR PARTICLE ACCELERATORS

R.G. Carter
Lancaster University, Lancaster, UK

Abstract

This paper reviews the main types of RF power amplifiers used for particle accelerators. It covers solid-state devices, tetrodes, inductive output tubes, klystrons, and gyrotrons with power outputs greater than 10 kW CW or 100 kW pulsed at frequencies from 50 MHz to 50 GHz. Factors affecting the satisfactory operation of amplifiers, including cooling, matching, and protection circuits, are discussed. The paper concludes with a summary of the state of the art for the different technologies.

1 INTRODUCTION

Many particle accelerators use high-power RF sources [1]. These sources must usually be amplifiers in order to achieve sufficient frequency and phase stability. The frequencies employed range from about 50 MHz to 50 GHz or higher. Power requirements range from 10 kW to 2 MW or more for continuous sources and up to 150 MW for pulsed sources. When sufficient power cannot be obtained from a single amplifier then the output from several amplifiers may be combined. In some cases power is supplied to a number of accelerating cavities from separate power amplifiers fed from a single low-power source. Other important factors include power conversion efficiency reliability and, in some cases, bandwidth.

Several types of power amplifier exist. The two main categories are solid-state devices and vacuum tubes. The former can only yield quite low powers and large numbers must be operated in parallel to reach even the lowest power levels required for accelerators. The vacuum tubes most commonly used to power accelerators are tetrodes and klystrons. Newer devices including the diacrode, the Inductive Output Tube (IOT), the Multiple-Beam Klystron (MBK), and the gyrotron may find applications in future. This paper sets out to provide a review of these types of amplifier together with a discussion of some of the factors affecting their successful operation.

2 SOLID-STATE AMPLIFIERS

Solid-state power amplifiers for use at high frequencies employ silicon bipolar transistors, silicon MOSFETs or silicon carbide Static Induction Transistors (SIT). An indication of the capabilities of UHF and VHF power amplifiers can be obtained by studying the state of the art of television transmitters at these frequencies [2]. The amplifiers used for accelerators are sometimes commercially available television transmitters or derived from them. The power required is obtained by operating numerous transistors in parallel. Reference [3] describes a 30 kW UHF television transmitter comprising six 6 kW power amplifiers each made up of eight 800 W modules. Each module in turn has twelve 110 W bipolar power output transistors, making a total of 576 transistors. A further seven power transistors of the same type are used in the driver stages of each module. Table 1 shows the state of the art of the principal types of transistor used in the UHF band.

Table 1: Solid-state UHF transistors: state of the art

	Si bipolar	**Si MOSFET**	**SiC SIT**
Peak power (W)	175	100	280
Mean power (W)	40	45	70
Operating voltage (V)	26 to 32	28 to 50	65
UHF gain (dB)	8 to 11	13 to 16	9 to 10
Maximum junction temperature (°C)	150	150	225

It is claimed that solid-state amplifiers are more reliable than their vacuum-tube counterparts by a factor of as much as 2.5 [3]. Because many transistors are operated in parallel, the failure of one produces a negligible drop in power output. However, the transistors are operated close to their design limits and they are known to be vulnerable to accidental overloads. Appreciable power is dissipated in the combining circuits and provision may be made to isolate a device that fails so that it does not adversely affect the performance of others nearby. For this reason further increases in the power output of solid-state amplifiers must be achieved by improvements in the transistors rather than by increasing the number used. Other advantages claimed for solid-state amplifiers are their high stability, low maintenance requirements, absence of warm-up time and low voltage operation. The supply voltage is low enough to avoid the safety problems associated with the HT supplies of tube amplifiers. The penalty which must be paid for this is the need to supply and handle very large d.c. currents. The transmitter described above requires a total current of the order of 2000 A. Such currents require large bus-bars in which there will be appreciable ohmic losses. It is not easy to deduce information about the conversion efficiencies of solid-state television transmitters from published information. This is because the figures quoted are calculated for a standard TV test signal rather than for continuous high-power operation. The transistors are operated in class AB (see Section 3.2) and it appears that the overall efficiencies of the UHF amplifiers are around 40%.

3 TETRODE AMPLIFIERS

Tetrode vacuum tubes are well established as high-power RF sources in the VHF (30–300 MHz) band. Figure 1(a) shows a schematic diagram of a tetrode. The voltages of the anode (known as the 'plate' in the USA) and the screen grid are positive with respect to the cathode whereas that of the control grid is normally negative. The current of electrons emitted from the cathode surface is controlled by the field of the control grid modified by those of the other two electrodes. The screen grid, maintained at RF ground, prevents capacitive feedback from the anode to the control grid. Figure 1(b) shows the characteristic curves of a typical tetrode. It is clear that the anode current depends strongly on the control grid voltage in a non-linear fashion. This voltage is normally negative with respect to the cathode to prevent electrons being collected on the grid with consequent problems of heat dissipation. If the anode voltage falls below that of the screen grid then any secondary electrons liberated from the anode are collected by the screen grid. For this reason the characteristic curves show kinks in that region. When tetrodes are operated as power amplifiers the anode voltage is always greater than the screen grid voltage. The curves show that the anode current varies very slowly with changes in the anode voltage.

The arrangement of a 150 kW, 30 MHz tetrode is shown in Fig. 2 [4]. The construction is coaxial with the cathode inside and the anode outside. This arrangement is necessary to enable the anode to be cooled (see Section 8.1). The output power available from such a tube is limited by the maximum current density available from the cathode and by the maximum power density that can be dissipated by the anode. The length of the anode must be much less than the free-space wavelength of the signal to be amplified to avoid variations in the signal level along it. The perimeter of the anode must likewise be much less than the free-space wavelength to avoid azimuthal higher-order modes in the space between the anode and the screen grid. The spacings between the electrodes must be small enough for the transit time of an electron from the cathode to the anode to be much less than the RF period. If attempts are

made to reduce the transit time by raising the anode voltage then there may be flashover between the electrodes. Reference [5] is the standard text on gridded tubes.

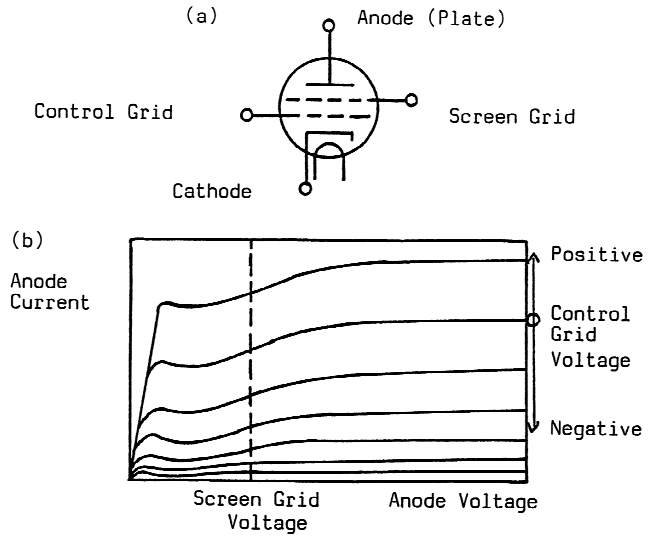

Fig. 1: Tetrode: (a) schematic diagram and (b) characteristic curves

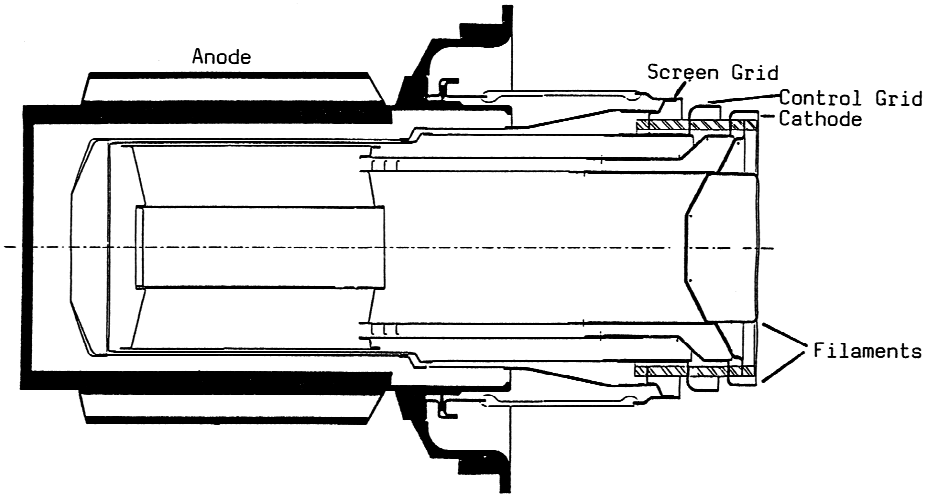

Fig. 2: Sectional view of a high-power tetrode (courtesy of Marconi Applied Technologies)

3.1 Tetrode amplifier circuits

Figure 3 shows the circuit of a grounded cathode tetrode amplifier with a tuned anode circuit. At lower frequencies a resistive anode load is used but this is unsatisfactory in the VHF band because of the effects of parasitic capacitance. The amplifiers used in accelerators are operated at a single frequency at any one time so the limited bandwidth of the tuned anode circuit is not a problem. At the resonant frequency the load in the anode circuit comprises the shunt resistance of the resonator (R_s) and the load resistance

(R_L) in parallel. If the load impedance has a reactive component then it merely detunes the resonator and can easily be compensated for. The d.c. electrode potentials are maintained by the power supplies shown and the capacitors provide d.c. blocking and RF bypass.

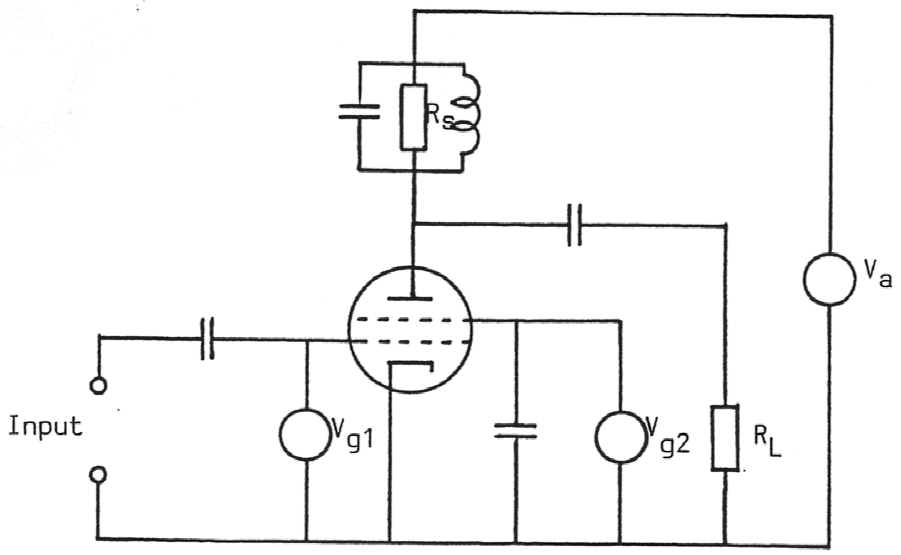

Fig. 3: Tetrode amplifier with grounded cathode

A commonly used alternative circuit is the grounded control grid circuit shown in Fig. 4. This circuit is not as simple to analyse as the previous one but it is easier to construct using tetrodes with the coaxial arrangement of electrodes shown in Fig. 2. Because both grids are at RF earth there is better isolation between the input and the output circuits. The other important difference is that in this circuit the full anode current flows in the input circuit, with the result that the input impedance and the gain are both lower than for the grounded cathode circuit.

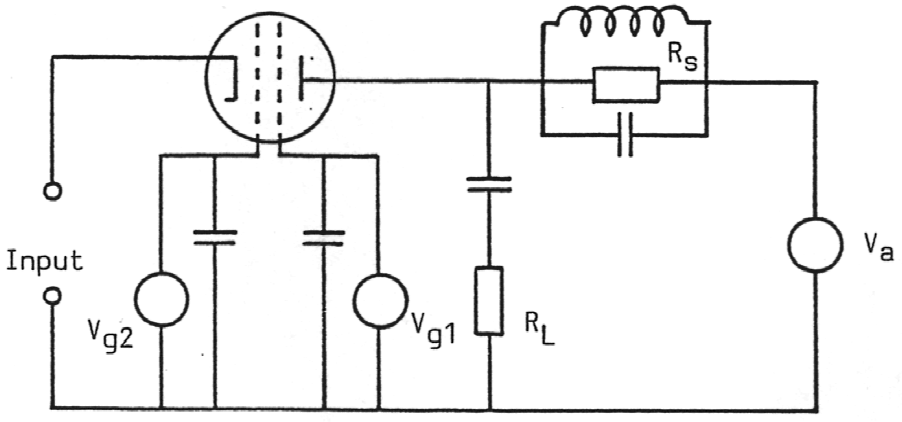

Fig. 4: Tetrode amplifier with grounded control grid

3.2 Classes of operation

Tuned amplifiers are normally operated in one of three modes, designated classes A, B, and C.

3.2.1 Class A

Figure 5(a) shows the form of the characteristic curves of a tetrode most commonly used for circuit design. The control grid voltage is plotted against the anode voltage with curves of constant anode, control grid, and screen grid currents shown. Because the anode circuit is tuned to the signal frequency the voltages on the two axes vary sinusoidally in antiphase with each other. The operation of the tube throughout the RF cycle is therefore represented by points on the straight load-line shown. In class A operation the tube conducts throughout the RF cycle, as shown in Fig. 5(b). The anode current curve is not quite a pure sinusoid because of the non-linearity of the tube characteristics. The ends of the load line are chosen so that the anode current is greater than or equal to zero at the maximum anode voltage and the control grid voltage is zero or slightly positive at the minimum anode voltage. The tube must then be biased so that in the absence of RF drive it sits at the quiescent ('Q') point shown at the centre of the load line.

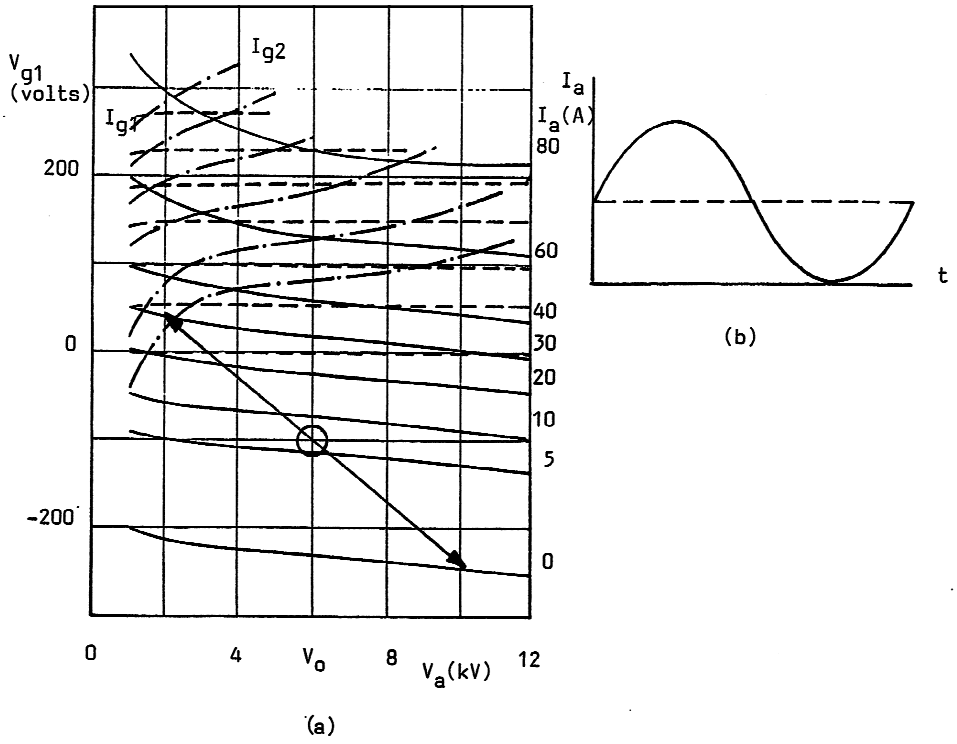

Fig. 5: Class A operation

This class of operation gives an output signal with low harmonic content, provided that the anode resonator does not have any higher-order modes that coincide with the harmonics of the signal frequency. The efficiency can be estimated easily if it is assumed that the amplifier is in linear operation with the anode current swinging from zero to I_{pk}. The mean anode current is then

$$I_0 = 0.5\, I_{\mathrm{pk}} \tag{1}$$

and the amplitude of the RF current is

$$I_1 = 0.5\, I_{\rm pk} \ . \tag{2}$$

If the minimum anode voltage is close to zero then the amplitude of the RF voltage is given by

$$V_1 = V_0 \ , \tag{3}$$

where V_0 is the anode voltage at the Q point. The d.c. power input to the tube is then

$$P_{\rm dc} = V_0\, I_0 = 0.5\, V_0\, I_{\rm pk} \tag{4}$$

and the RF power output is

$$P_{\rm rf} = 0.5\, V_1\, I_1 = 0.25\, V_0\, I_{\rm pk} \ . \tag{5}$$

From Eqs. (4) and (5) the efficiency is

$$\eta = P_{\rm rf}/P_{\rm dc} = 50\% \ . \tag{6}$$

The difference between the d.c. input and RF output powers is dissipated as heat in the anode. A more exact analysis, taking into account the non-linearity of the tube and the actual values of the voltages and currents, gives a lower figure for the efficiency. The calculation above therefore gives an upper limit for class A operation. If the tube is operated in class A then power is drawn from the supply and dissipated in the anode even when there is no RF drive and the tube is sitting at the Q point.

3.2.2 Class B

In class B operation the tube is biased so that the Q point lies on the curve of zero anode current. It then conducts only during the positive half-cycle of the control grid voltage. This is illustrated in Fig. 6. During the negative half-cycle of the control grid voltage the anode voltage swings to a voltage that is nearly twice that at the Q point because of the resonant output circuit. The anode current waveform has a higher harmonic content than in class A operation.

The estimation of the efficiency of the amplifier follows the same pattern as in the previous Section. Assuming that the tube is linear while it is conducting, the mean and RF currents can be found by Fourier analysis of the waveform in Fig. 6(b):

$$I_0 = I_{\rm pk}/\pi \tag{7}$$

and

$$I_1 = 0.5\, I_{\rm pk} \ , \tag{8}$$

while

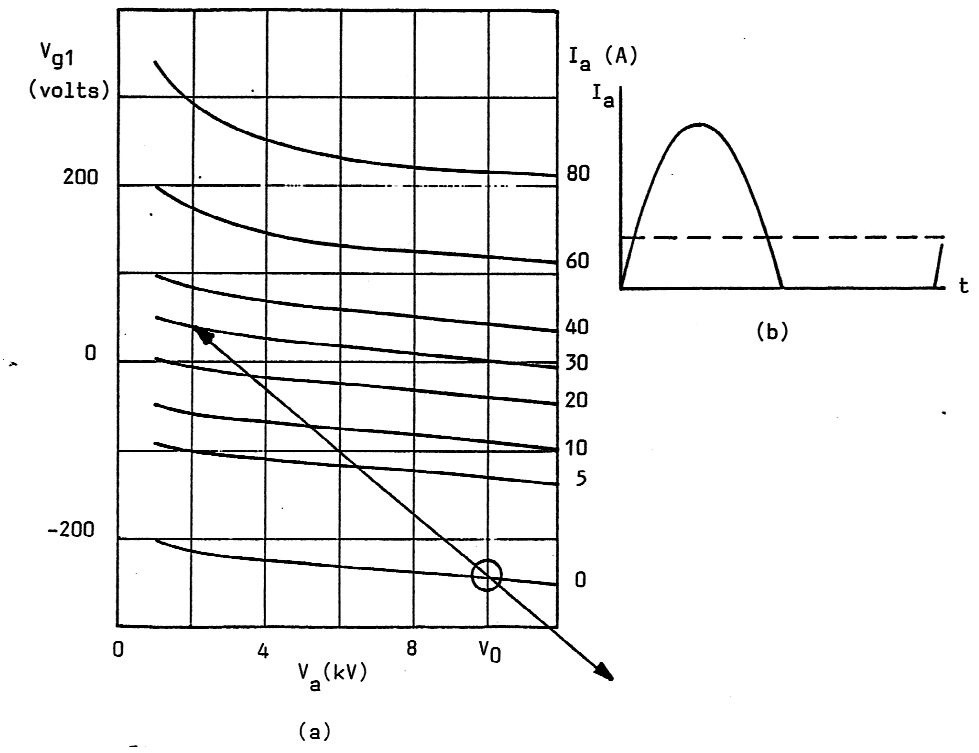

Fig. 6: Class B operation

$$V_1 = V_0 \tag{9}$$

as before. The d.c and RF powers are given by

$$P_{\rm dc} = V_0\, I_0 = V_0\, I_{\rm pk}/\pi \tag{10}$$

and

$$P_{\rm rf} = 0.5\, V_1\, I_1 = 0.25\, V_0\, I_{\rm pk} \ . \tag{11}$$

Comparison of Eqs. (10) and (11) with Eqs. (4) and (5) shows that the d.c. power is proportionately less in this case because the mean anode current is lower. The efficiency is

$$\eta = \pi/4 = 78.5\% \ . \tag{12}$$

This, again, is the upper limit of the possible efficiency of this class of operation. The example in Section 3.3 shows the effect of taking non-linearity and other imperfections into account. Devices are sometimes operated in a regime between classes A and B and this is described as class AB operation. It represents a compromise between the requirements of low harmonic content and high efficiency.

3.2.3 Class C

In class C operation the tube is biased so that it is cut off for more than half of the RF cycle, as shown in Fig. 7. If it is assumed that the tube operation is linear when it is conducting, then the efficiency can be estimated by the same method as before. For example if the angle of conduction is 90° then

$$I_0 = 0.165\, I_{\rm pk} \ , \tag{13}$$

$$I_1 = 0.31\, I_{\rm pk} \ , \tag{14}$$

$$V_1 = V_0 \tag{15}$$

and

$$P_{\rm dc} = 0.165\, V_0\, I_{\rm pk} \ . \tag{16}$$

So

$$P_{rf} = 0.5\, V_1\, I_1 = 0.155\, V_0\, I_{\rm pk} \tag{17}$$

and

$$\eta = 94\% \ . \tag{18}$$

Evidently the efficiency increases as the conduction angle decreases, but with the penalty of greater non-linearity and higher harmonic content in the output waveform. The other penalty to be paid for this increase in efficiency is a reduction in gain because the tube must be driven harder. This is not a serious penalty because the power consumed by the driver stages of the amplifier is a small proportion of the whole power consumption.

3.3 Tetrode amplifier design

The process by which a tetrode amplifier can be designed is best explained by means of an example. This is based upon a 62 kW, 200 MHz amplifier used in the CERN SPS [6]. The example was chosen because sufficient information is available about the amplifier to verify the results of the calculations. The amplifier uses a single RS2058CJ tetrode [7] operating with a d.c. anode voltage of 10 kV and 900 V screen grid bias. The design procedure described below is based upon that given in Ref. [8].

The actual amplifier is operated in class AB, but quite close to class B. For simplicity we will assume class B operation in the calculations that follow. The first stage is to estimate the probable efficiency of the amplifier. We know that this must be less than the theoretical limit given in Eq. (12) so let us try 75%. Then the d.c. power input necessary to obtain the desired output power is

$$P_{\rm in} = 62/0.75 = 83\,{\rm kW} \ . \tag{19}$$

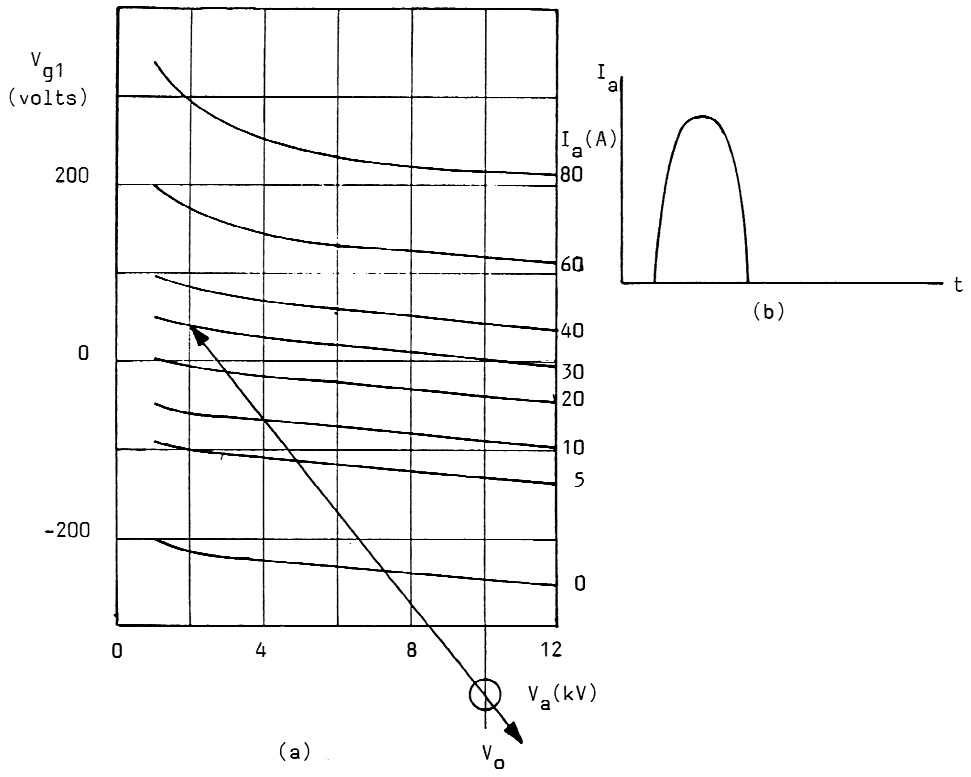

Fig. 7: Class C operation

The d.c. anode voltage was chosen to be 10 kV so the d.c. anode current is

$$I_0 = 83/10 = 8.3\,\mathrm{A} \quad . \tag{20}$$

The theoretical value of I_{pk} is given by Eq. (7) but Ref. [8] suggests that a factor of 3.5 to 4.5 should be taken as a first estimate of the ratio of the currents in place of π because of the non-linearity of the tube. If we take the factor to be 4.0 then

$$I_{\mathrm{pk}} = 40 \times 8.3 = 33\,\mathrm{A} \quad . \tag{21}$$

Next we construct the load line on the characteristic curves for the tube shown in Fig. 8 by choosing the minimum anode voltage. To ensure that the anode voltage is always greater than the screen grid voltage we select a value of 1.5 kV. The left-hand end of the load line is then fixed by this voltage and the peak anode current of 33 A, as shown in Fig. 8. We note that this requires the control grid voltage to swing slightly positive with a maximum of 60 V.

To find the anode current waveform we carry out the construction shown in the lower part of Fig. 8. The radius of the arc is equal to the length of the load line from the Q point to one end. From the arc we construct lines from which the anode current can be found at 15° phase intervals of the anode voltage. The results are shown in Table 2.

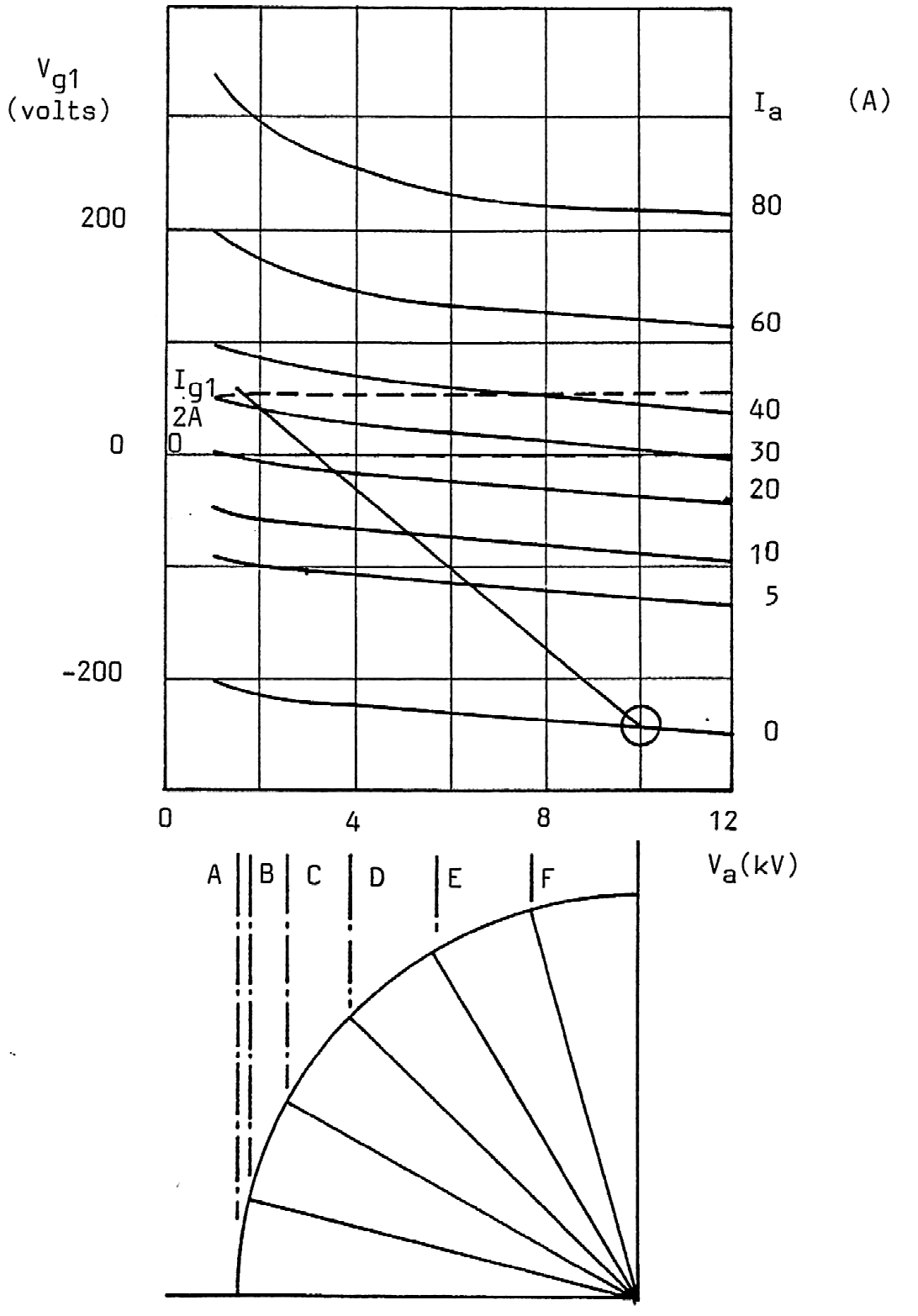

Fig. 8: RS 2058 CJ characteristic curves (courtesy of Siemens AG)

Table 2: Anode currents at 15° phase intervals taken from Fig. 8

Point	**Degrees**	I_a **(A)**
A	0	33
B	15	32
C	30	27
D	45	18
E	60	8
F	75	3

The d.c. and RF anode currents can be found by Fourier analysis of the current waveform using the numerical formulae given in Ref. [8]:

$$I_0 = (0.5\,A + B + C + D + E + F)/12 \tag{22}$$

and

$$I = (A + 1.93\,B + 1.73\,C + 1.41\,D + E + 0.52\,F)/12 \ . \tag{23}$$

When these formulae are used with the data from Table 2 the results are:

$$I_0 = 8.7\,\mathrm{A} \tag{24}$$

and

$$I_1 = 14.7\,\mathrm{A} \ . \tag{25}$$

The figures given by Eqs. (24) and (25) can be compared with the values of 8.3 A and 10.5 A given by Eqs. (20) and (7), respectively. The amplitude of the RF voltage is

$$V_1 = 10.0 - 1.5 = 8.5\,\mathrm{kV} \ . \tag{26}$$

The d.c. input power is then

$$P_{\mathrm{dc}} = 10.0 \times 8.7 = 87\,\mathrm{kW} \tag{27}$$

and the RF output power is

$$P_{\mathrm{rf}} = 0.5\,V_1\,I_1 = 62.5\,\mathrm{kW} \ , \tag{28}$$

which is very close to the desired value. The efficiency is 72%, which is slightly less than the value originally assumed. We can also calculate the input and output resistances of the tube. The output resistance is

$$R_{\text{out}} = V_1/I_1 = 5/8\ \Omega\ . \tag{29}$$

To find the input impedance we note that the amplitude of the RF control grid voltage is

$$V_{\text{in}} = 245 + 60 = 305\,\text{V}\ , \tag{30}$$

and that for grounded grid operation the RF input current is

$$I_{\text{in}} = I_1 + I_{g1} = 14.7 + 0.6 = 15.3\,\text{A}\ , \tag{31}$$

where the control grid current I_{g1}, is obtained by reading the control grid currents off Fig. 8 at 15° intervals and employing Eq. (23). Then the RF input resistance is

$$R_{\text{in}} = V_{\text{in}}/I_{\text{in}} = 20\,\Omega\ . \tag{32}$$

Finally we note that the input power is

$$P_{\text{in}} = 0.5\,V_{\text{in}}\,I_{\text{in}} = 2333\,\text{W} \tag{33}$$

and that the power gain of the amplifier is

$$\text{Gain} = 10\ \log(62.5/2.3) = 14.3\,\text{dB}\ . \tag{34}$$

Table 3 shows a comparison between the figures calculated above and those reported in Ref. [6]. The differences between the two columns of Table 3 are entirely attributable to the difference between the actual class AB operation and the class B operation assumed in the calculations.

Table 3: Comparison between actual and calculated parameters of the amplifier described in Ref. [6]

Parameter	**Actual**	**Calculated**	**Units**
V_0	10	10	kV
I_0	9.4	8.7	A
V_{g2}	900	900	V
V_{g1}	– 200	– 245	V
I_{g1}	105	600	mA
P_{out}	62	62.5	kW
P_{in}	1.8	2.3	kW
Gain	15.4	14.3	dB
η	64	72	%

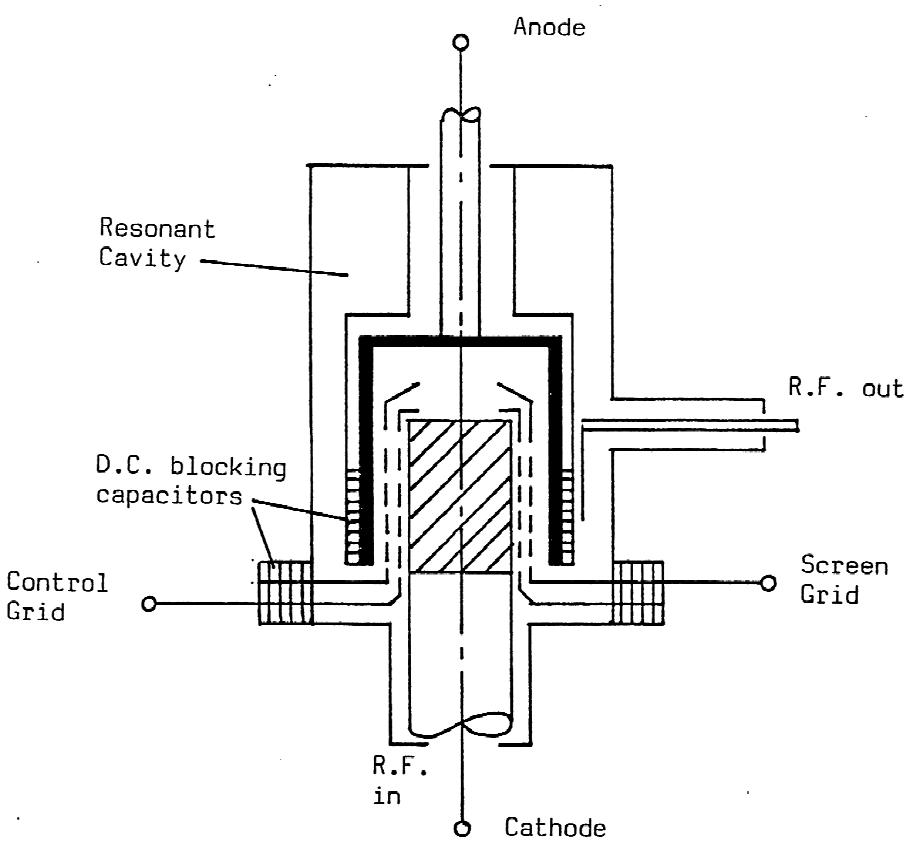

Fig. 9: Arrangement of a tetrode amplifier

3.4 Practical details

Figure 9 shows a simplified diagram of the arrangement of the tetrode amplifier for the RIKEN ring cyclotron described in Ref. [9]. The tube is operated in the grounded grid configuration with coaxial input and output circuits. The outer conductors of the coaxial lines are at ground potential and they are separated from the grids by d.c. blocking capacitors. The anode resonator is a re-entrant coaxial cavity, which is separated from the anode by a d.c. blocking capacitor. The output power is coupled through an impedance matching device to a coaxial line. The anode HT connection and water cooling pipes are brought in through the centre of the resonator.

The electrodes of the tube form coaxial lines with characteristic impedances of a few ohms. We have seen above that the input impedance of the amplifier is typically a few tens of ohms and the output impedance a few hundred ohms. Thus both the input and output lines are terminated in near open-circuit loads. The anode resonator therefore has one end open circuited and the other short circuited and it must be an odd number of quarter wavelengths long at resonance. Typically the resonator is 3/4 of a wavelength long. In this case the point at which the output coaxial line is brought into the resonator can be used to transform the impedance to provide a match. There is also a voltage node towards the lower end of the outer part of the resonator, and this can be used to bring connections through to the anode [10]. The higher-order modes of the cavity can be troublesome and it is usually necessary to damp them by the selective placing of lossy material or of coupling loops connected to external loads within the cavity [6, 9–11]. The tube heater connections must incorporate some means of decoupling from the RF circuit [6, 9].

It will be clear from what has already been said that the tube input and output are mismatched to the external connections. It is therefore necessary to devise matching networks for these connections. Figure 10(a) shows a simplified form of the input circuit of the amplifier discussed in Section 3.3. The source (normally 50 Ω) feeds the tube through a length of low impedance coaxial line. The line is terminated by the tube input impedance shunted by the capacitance between the control grid and the cathode. For the RS2058CJ tetrode this capacitance is 140 pF so that it has a reactance of 5.7 Ω at 200 MHz. This is comparable with the input resistance of 20 Ω so its effect must be allowed for. In practice the connecting coaxial line is made up of several sections having different impedances [9, 10].

Figure 10(b) shows the output circuit of the amplifier. The output resistance is shunted by the capacitance between the screen grid and the anode, which is 40 pF, with a reactance of 20 Ω at 200 MHz in this case. The tube is connected to the coaxial cavity resonator by a coaxial line and the load is connected by another line and, possibly, an impedance matching network. The effect of the anode/screen grid capacitance will normally be to tune the frequency of the cavity somewhat. Variations in the load impedance may have a similar effect, which can be compensated for by tuning the cavity. They may also require a variable matching network so that the load can be kept correctly matched to the amplifier [6, 9, 10]. If the impedance presented to the anode is too high the anode voltage swing may be excessive with the possibility of damage to the tube through internal arcing.

3.5 Operation of tetrode amplifiers in parallel

When higher powers are required than can be obtained from a single tube, it is then possible to operate several tubes in parallel. Two such systems are described in Ref. [11]. The original four 500 kW, 200 MHz power amplifiers for the CERN SPS each comprised four 125 kW tetrodes operating in parallel. Figure 11 shows the arrangement of one amplifier. The loads on the fourth arms of the 3 dB couplers normally receive no power. If one tube fails, however, they must be capable of absorbing the power from the unbalanced coupler. The amplifier also contains coaxial transfer switches (not shown in Fig. 11), which make it possible for a faulty tube to be completely removed from service. The remaining three tubes can then still deliver 310 kW to the load. A more recent design of a 500 kW amplifier for the same accelerator employs sixteen 35 kW units operated in parallel, with a seventeenth unit as the driver stage. Both types of amplifier operate at anode efficiencies greater than 55% and overall efficiencies greater than 45%.

3.6 The Diacrode®

A recent development of the tetrode is the Diacrode[1] [12, 13]. In this tube the coaxial line formed by the anode and the screen grid is extended to a short circuit, as shown in Fig. 12. The consequence of this change is that the standing wave now has a voltage antinode and a current node at the centre of the active region of the tube. The tetrode, in contrast, has a voltage antinode and current node just beyond the end of the active region, as shown in Fig. 12. Thus, for the same RF voltage difference between the anode and the screen grid, the Diacrode has a smaller reactive current flow and much smaller power dissipation in the screen grid than a tetrode of similar dimensions. This means that, compared with conventional tetrodes, Diacrodes can either double the output power at a given operating frequency or double the frequency for a given power output. The gain and efficiency of the Diacrode are the same as those of a conventional tetrode. Table 4 shows the comparison between the TH 526 tetrode and the TH 628 Diacrode operated at 200 MHz.

[1] The name Diacrode is the registered property of Thomson Tubes Electroniques.

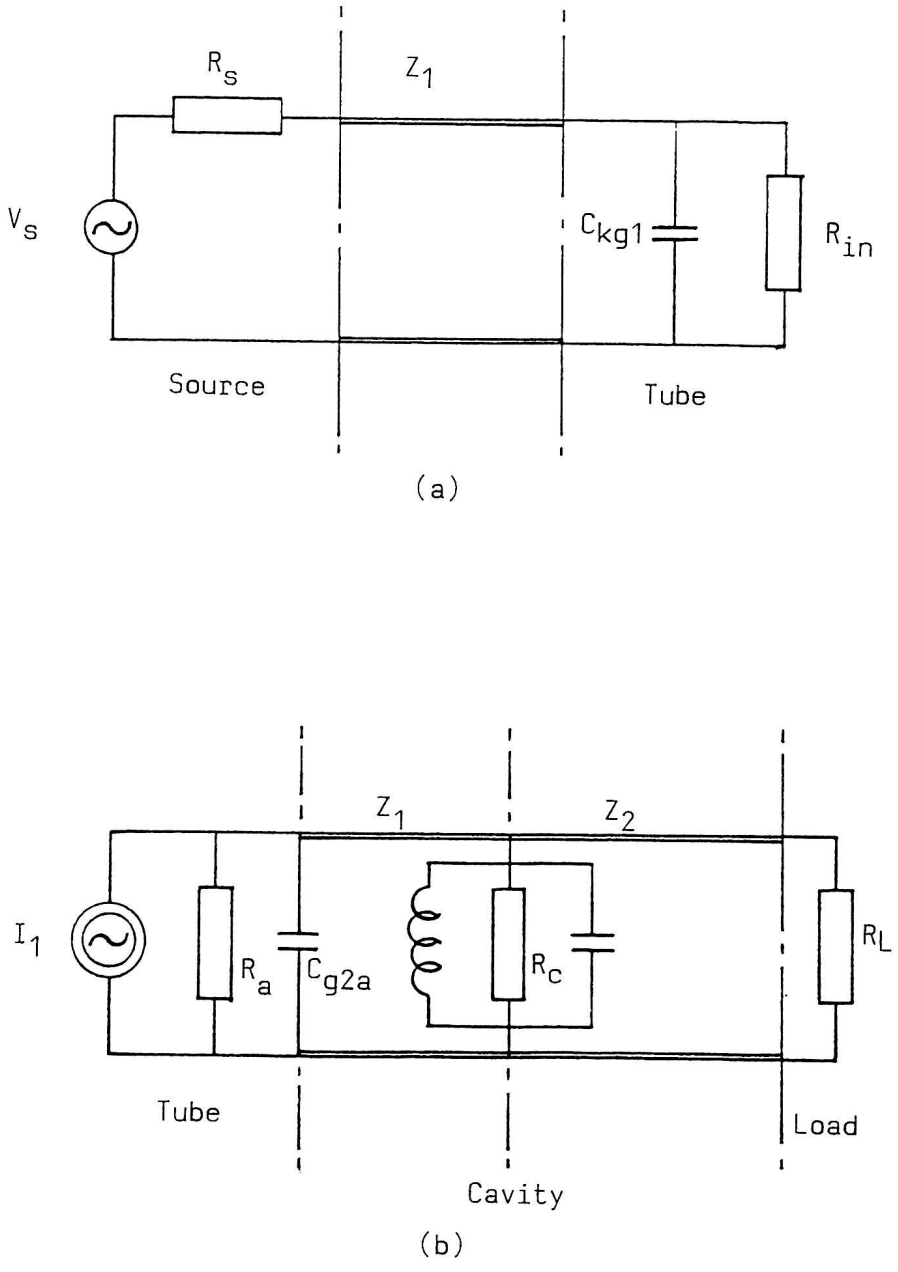

Fig. 10: Tetrode amplifier: (a) input circuit and (b) output circuit

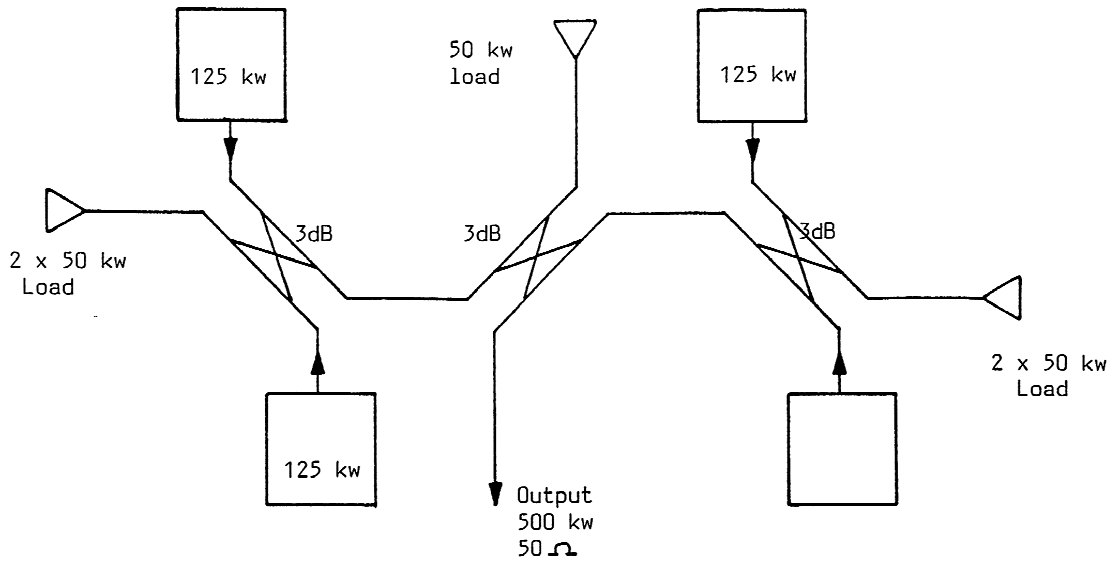

Fig. 11: Parallel operation of tetrode amplifiers

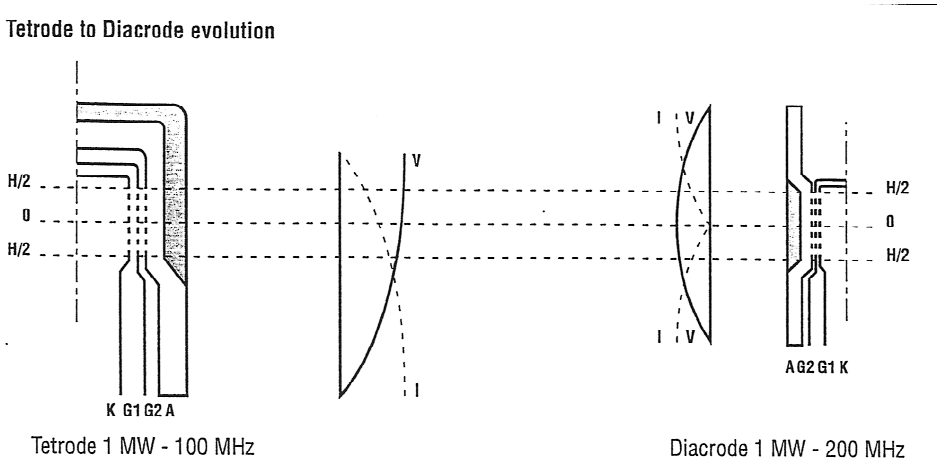

Fig. 12: Comparison between a tetrode and a Diacrode (courtesy of Thales)

Table 4: Comparison between the TH 526 tetrode and the TH 628 Diacrode

Parameter	**Units**	**TH 526**	**TH 628**
Pulse duration	ms	2.2	2.5
Peak output power	kW	1600	3000
Average output power	kW	240	600
Anode voltage	kV	24	26
Anode current	A	124	164
Peak input power	kW	64.9	122.5
Gain	dB	13.9	13.9

4 INDUCTIVE OUTPUT TUBES

The tetrode suffers from the disadvantage that the same electrode, the anode, is part of both the d.c. and the RF circuits. The output power is, therefore, limited by grid and anode dissipation. To get high power at high frequencies it is necessary to employ high velocity electrons and to have a large collection area for them. It is therefore desirable to separate the electron collector from the RF output circuit. The possibility that these two functions might be separated from each other was originally recognized by Haeff in 1939, but it was not until 1982 that a commercial version of this tube was described [14]. Haeff called his invention the Inductive Output Tube (IOT) but it is also commonly known by the proprietary name Klystrode®[2]. The basis of operation of the IOT is illustrated in Fig. 13, which shows how a current is induced in a resonant cavity by the azimuthal magnetic field of a bunch of electrons passing through it (hence the name of the tube). The bunches of electrons can be produced by a high-voltage electron gun and the spent beam can be collected on an electrode with a large surface area.

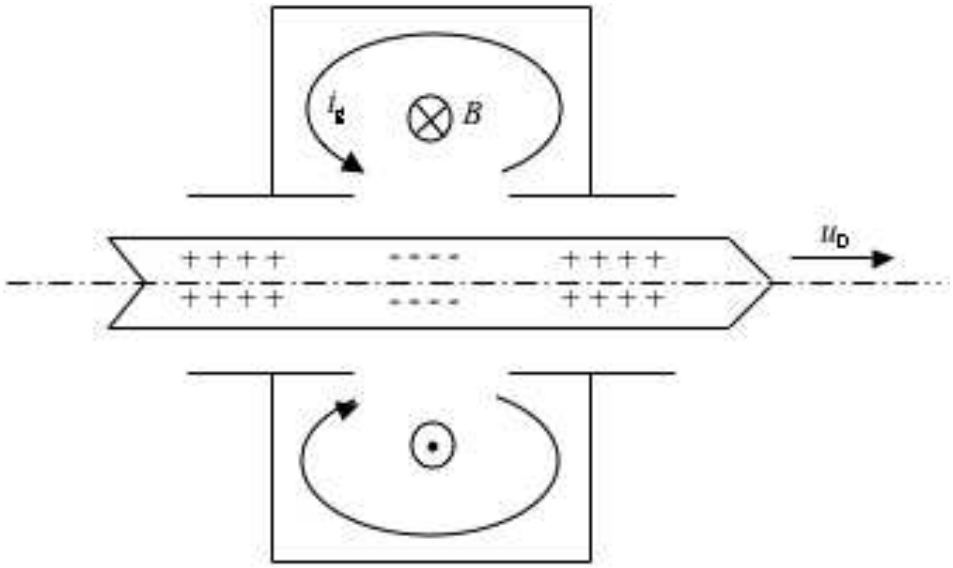

Fig. 13: Current induced in a cavity resonator by a bunched electron beam

Figure 14 shows a schematic diagram of an IOT. The electron beam is formed by a gridded, convergent-flow electron gun and confined by an axial magnetic field (not shown). The gun is biased so that no current flows except during the positive half-cycle of the RF input. The resulting bunches of electrons excite the cavity resonator in a manner analogous to class B or class C amplifier operation. The operation of this tube can be understood by comparing it with that of a tetrode, as shown in Fig. 15. In this figure the solid lines show the potentials at the peak of the current flow, and the broken lines show them when there is no current flowing. In a tetrode amplifier the anode voltage is lowest at maximum anode current so the electrons cross the tube relatively slowly. The gap between the screen grid and the anode must therefore be kept small to minimize transit time effects and the peak anode voltage is, accordingly, limited. In the IOT the electrons enter the gap with high velocity and encounter an opposing electric field which extracts energy from them and transfers it into the RF fields in the cavity resonator. Since the electron velocity is high it is possible to use a much longer output gap than in the tetrode.

Advantages of the IOT are that it does not need a d.c. blocking capacitor in the RF output circuit since the cavity is at ground potential, and it has higher isolation between input and output and a longer life than an equivalent tetrode. These advantages are offset to some extent by the need for a magnetic focusing field. The typical gain is 24 dB, which is appreciably higher than that of a tetrode; high enough

[2] The name Klystrode is the registered property of CPI Inc.

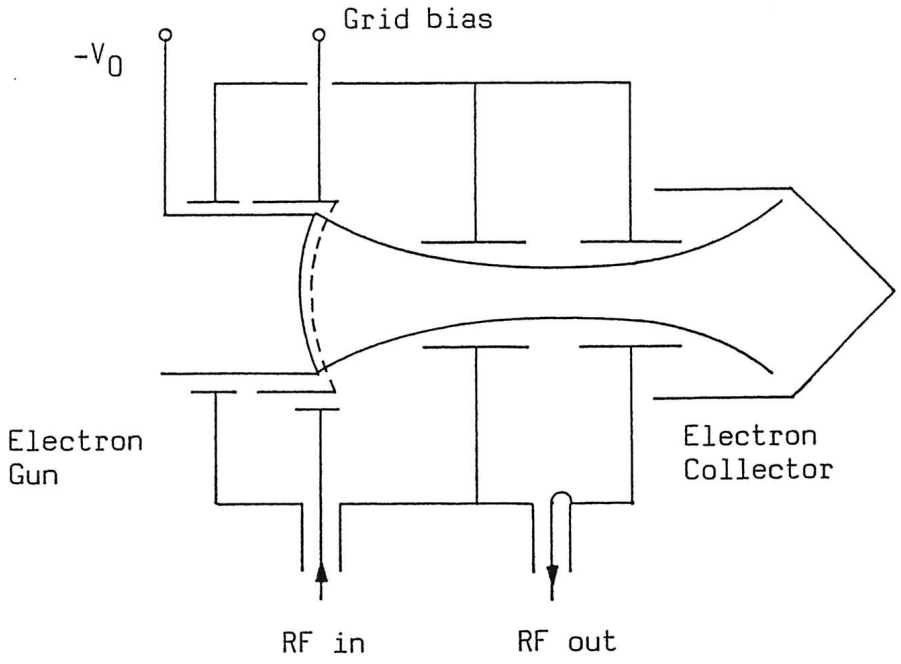

Fig. 14: Schematic diagram of an inductive output tube

in fact for a 60 kW tube to be fed by a solid-state driver stage. The IOTs designed for television service are operated in class B and have dual input and output cavities to give the necessary bandwidth. Tubes currently available give up to 60 kW of power in the UHF TV bands (470–860 MHz). In principle the efficiency can be still further enhanced by collector depression (see Section 5.3.1). A tube for use in an accelerator does not need to have the additional cavities and can operate in class C with an efficiency of around 70%. It has been suggested that IOTs could be useful from about 100 MHz to perhaps 3 GHz with CW powers up to 1 MW at the lower frequencies and some tens of kilowatts at the higher frequencies. Further information about the IOT can be found in Refs. [14] and [15].

5 KLYSTRONS

At frequencies of 300 MHz and above the power sources for accelerators are generally klystrons. The klystron extracts power from a bunched electron beam in the same manner as an IOT, but the bunches are produced by velocity modulation of the beam rather than by switching it on and off. Figure 16 shows a schematic diagram of a two-cavity klystron. Most klystrons used for accelerators have four, five, or even more cavities in order to get high gain and the highest possible efficiency. The long, high-current electron beam is confined by an axial magnetic field throughout the interaction region.

5.1 Electron bunching in klystrons

The method by which the electron beam in a klystron is velocity modulated is illustrated in Fig. 17. The beam passes through a cavity resonator, very like the output cavity of an IOT, which is excited in the TM_{010} mode so that there is an axial electric field across the gap in the drift tube. The electrons are accelerated or retarded according to the phase of the RF field in the gap as they cross it. As the beam leaves this cavity it is velocity modulated, but there is no current modulation.

Figure 18 shows the way in which the velocity modulation produces electron bunches. The motion of a number of sample electrons is displayed in a frame of reference, which is moving at the initial beam velocity. The peak accelerating phase is marked $\oplus$ and the peak retarding phase is marked O. Those

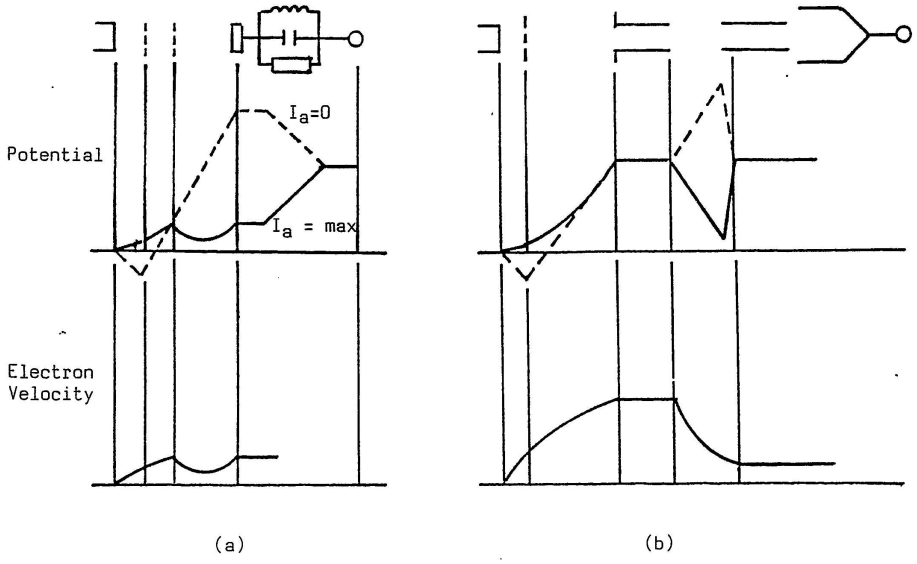

Fig. 15: Comparison between (a) tetrode and (b) IOT operation

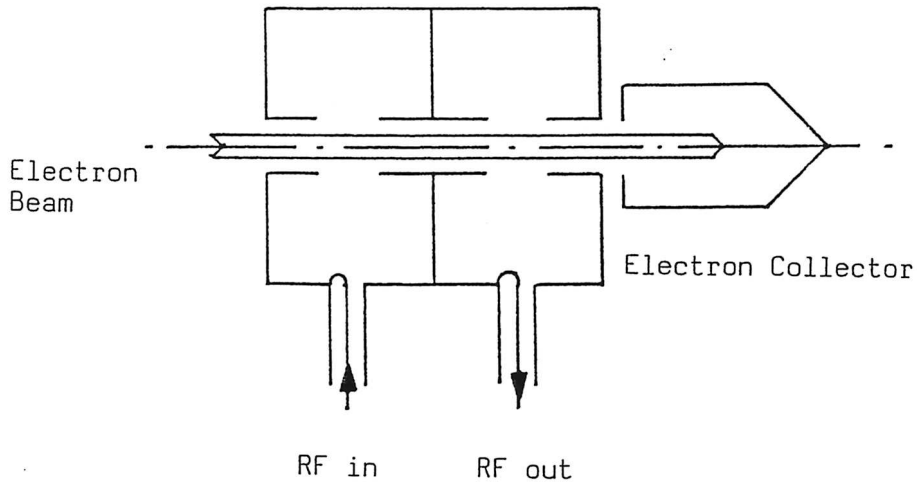

Fig. 16: Schematic diagram of a two-cavity klystron

electrons which cross the input gap at an instant when the field is zero proceed without any change in their velocities and appear as horizontal straight lines. Retarded electrons move upwards and accelerated electrons move downwards in the diagram. The velocity modulation causes the electrons to become bunched together until further bunching is prevented by the space-charge repulsion between the electrons. Under small-signal conditions the beam has current modulation but no velocity modulation at the plane of the bunch. Figure 18 is an example of an Applegate diagram. In a simple klystron (Fig. 17) a second cavity, tuned to the signal frequency, is placed at the plane of maximum bunching. This cavity presents a resistive impedance to the current induced in it by the electron beam, so the phase of the field across the gap is in anti-phase with the RF beam current. Electrons that cross the gap within $\pm$ 90° of the bunch centre are retarded and give up energy to the field of the cavity. Since more electrons cross the second gap during the retarding phase than the accelerating phase there is a net transfer of energy to the RF field of the cavity. Thus the klystron operates as an amplifier by converting some of the d.c. energy

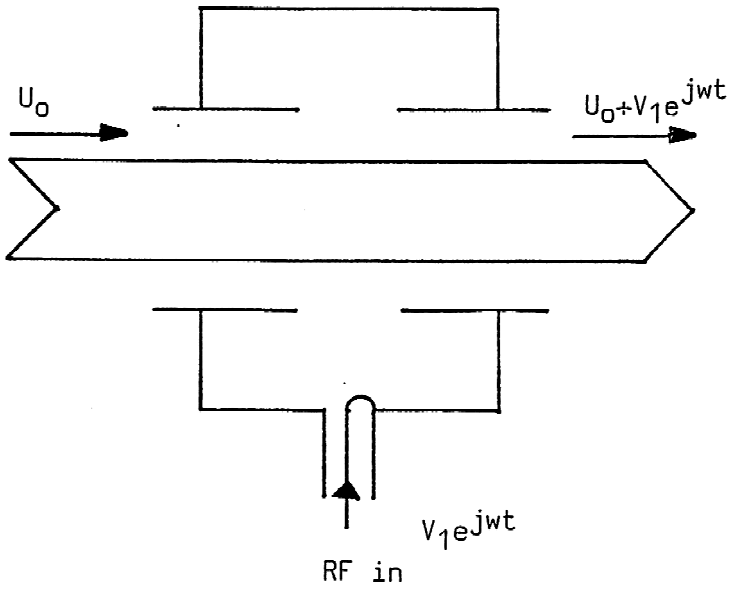

Fig. 17: Velocity modulation of an electron beam by a cavity resonator

input into RF energy in the output cavity. If the second cavity were removed the electron bunches would disperse under the influence of space-charge, only to re-form further down the tube. Under small-signal conditions this process is repeated periodically. From the point of view of an observer travelling with the mean electron velocity the electrons would appear to be executing oscillations about their mean positions at the electron plasma frequency. The plasma frequency is modified to some extent by the boundaries surrounding the beam and by the presence of the magnetic focusing field.

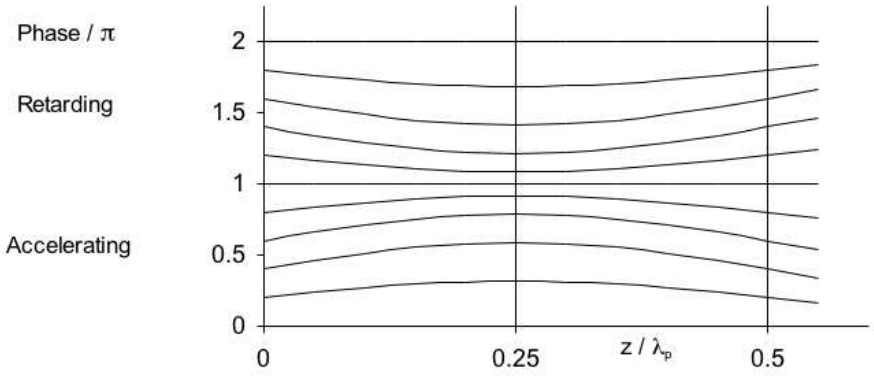

Fig. 18: Bunching of a velocity modulated electron beam

The electron plasma frequency is given by

$$\omega_p = (\eta\rho/\varepsilon_0)^{0.5} \quad , \tag{35}$$

where η is the charge-to-mass ratio of the electron and ρ is the charge density in the beam. The distance

from the input gap to the first plane at which the bunching is maximum is then a quarter of a plasma wavelength (λ_p), given by

$$\lambda_p = 2\pi u_0/\omega_p \tag{36}$$

where u_0 is the mean electron velocity.

The bunching length is independent of the input signal except at very high drive levels, when it is found that the bunching length is reduced. If attempts are made to drive the tube still harder the electron trajectories cross over each other and there is less bunching. The transfer characteristic of a klystron (Fig. 19) shows that the device is a linear amplifier at low signal levels but that the output saturates at high signal levels. A tube used in an accelerator would normally be run at, or close to, saturation to obtain the highest possible efficiency.

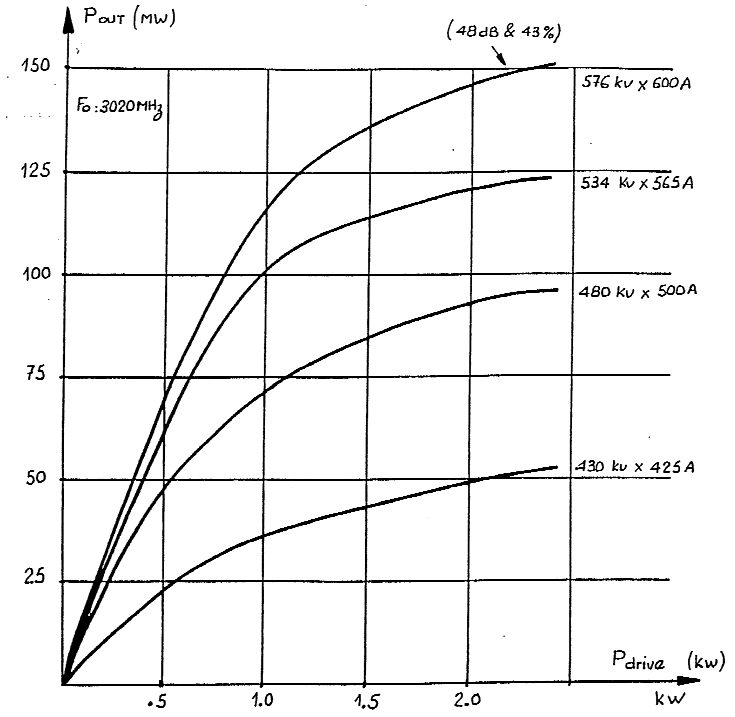

Fig. 19: Klystron transfer characteristics (courtesy of Thales)

5.1.1 The effect of bunching on efficiency

The conversion efficiency of a klystron depends upon the interaction between the bunched beam and the electric field of the output cavity. This is illustrated in Fig. 20, which shows the waveform of the output gap field (assumed to be sinusoidal) and a number of possible current waveforms [16]. To simplify the discussion we assume that the electrons in the bunch all have the same energy V_0 electron volts and that the magnitude of the output gap voltage V_g is equal to V_0, as shown in Fig. 20(a). It follows that any electron that crosses the gap when the field is at its maximum and retarding loses all its energy to the field if transit time effects are neglected.

It used to be supposed that the maximum conversion efficiency would be obtained by maximizing the amplitude of the fundamental harmonic component of the beam current. It can be shown that the ratio of the RF current i_1, to the mean current I_0, is 1.16. Figure 20(b) shows the normalized RF beam current

when the ratio is 1.0 and no higher harmonics are present. Only a small proportion of the electrons cross the gap when the field is close to its maximum retarding value, and those in the shaded region of the diagram experience an accelerating field and remove energy from the cavity. The instantaneous power flow from the beam to the cavity, normalized to the d.c beam power, is

$$P/P_0 = \frac{i_g V_g}{I_0 V_0} = \cos\theta\,[1 + \cos\theta] \quad , \tag{37}$$

where θ is the phase angle of the field. The mean power and hence the efficiency are obtained by integrating Eq. (38) over one RF cycle to give

$$\eta = \frac{1}{2\pi}\int_0^{2\pi} \cos\theta\,[1 + \cos\theta]\,d\theta = 0.5 \quad . \tag{38}$$

The theory of klystron bunching that ignores the effects of space-charge predicts the optimum current waveform shown in Fig. 20(c). In this case some electrons also cross the gap at an accelerating phase of the field. A calculation along the lines of that above shows that the maximum possible efficiency is 58%. The identical figure is given by the calculation above if i_g/I_0 is assumed to be 1.16.

Figures 20(d) and 20(e) show two possible waveforms in which all the electrons cross the gap when the field is retarding. The waveform in Fig. 20(d), which is analogous to class B operation of a tetrode, produces an efficiency of 71%, whereas that in Fig. 20(e) gives 90%. When the effects of circuit losses are considered it is evident from the efficiencies measured that high-power klystrons commonly operate under conditions close to those of Fig. 20(e) (see Section 5.3).

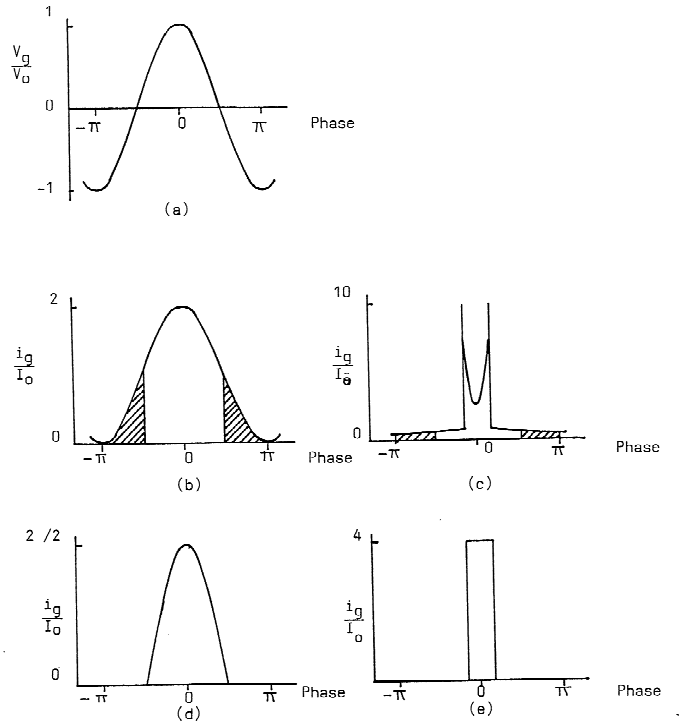

Fig. 20: Klystron output gap waveforms (courtesy of H. Bohlen)

5.1.2 Formation of bunches

Figure 18 shows that the tightness of the bunches formed by velocity modulation is limited by space-charge forces. It follows that it is easiest to obtain high efficiency with a beam in which the current density is low and the velocity is high, that is, with a low perveance ($I_0/V_0^{1.5}$). Figure 21 shows the effect of perveance on efficiency for a particular klystron.

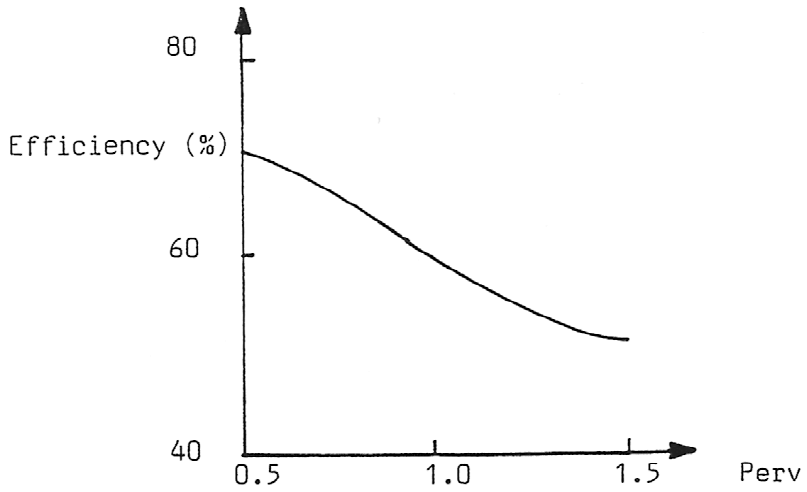

Fig. 21: Dependence of the efficiency of a klystron on the beam perveance

Figure 22 shows the Applegate diagram computed for a typical super-power klystron [17]. The tube has five cavities placed as shown, and the peak accelerating and retarding fields are marked in the same way as before. The bunching produced by the first cavity is imperceptible on the scale of this diagram but it is sufficient to excite the RF fields in the second cavity. The second cavity is tuned to a frequency above the signal frequency so that it presents an inductive impedance to the beam current. As a result the bunch centre coincides with the neutral phase of the field in the cavity and further velocity modulation is added to the beam, which produces much stronger bunching at the third cavity. The third cavity is tuned to the second harmonic of the signal frequency, as can be seen from a careful examination of the diagram. The principal purpose of this cavity is to cause the electrons lying farthest from the bunch centre to be gathered into the bunch. The use of a second harmonic cavity increases the efficiency of a klystron by at least ten percentage points. The splitting of the lines in the diagram that occurs at this plane is caused by a divergence in the behaviour of electrons in different radial layers within the electron beam. The fourth cavity is similar to the second cavity and produces still tighter bunching of the electrons. By the time they reach the final cavity nearly all the electrons are bunched into a phase range which is $\pm$ 90° with respect to the bunch centre. The output cavity is tuned to the signal frequency so that the electrons at the bunch centre experience the maximum retarding field and all electrons that lie within a phase range of $\pm$ 90° with respect to the bunch centre are also retarded. If the impedance of the output cavity is chosen correctly then a very large part of the bunched beam's kinetic energy can be converted into RF energy. Computer simulations have shown that the ratio of the fundamental beam RF current to the d.c. beam current can be as high as 1.6 to 1.7 at the output cavity.

5.2 Terminal characteristics of klystrons

The performance of a klystron is appreciably affected by variations in beam voltage, signal frequency, and output match, and we now examine these in turn.

Klystrons for use in accelerators are normally operated at or close to saturation. Figure 19 shows that the output power is then insensitive to variations in input power and, by extension, to variations in

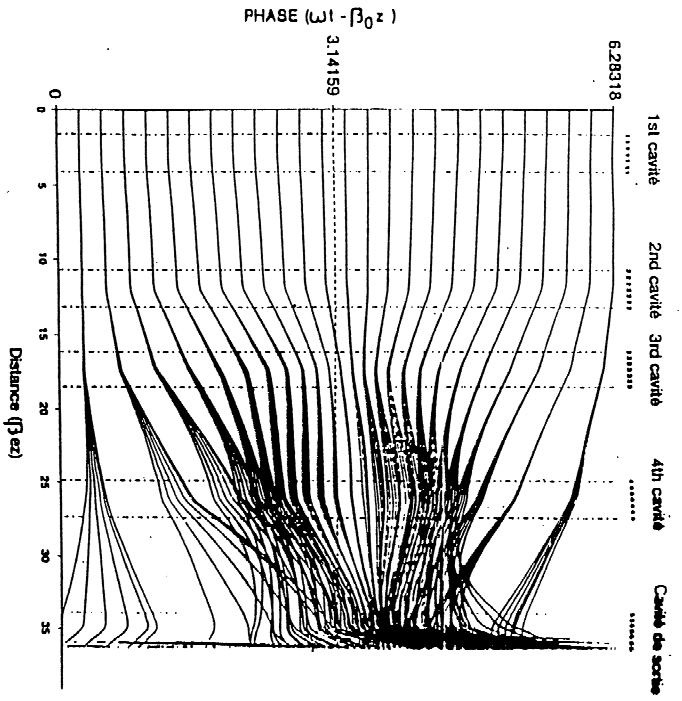

Fig. 22: Electron bunching in a high power five-cavity klystron (courtesy of Thales)

beam voltage. The effects on the phase of the output signal are more serious because of the distance from the input to the output. If the distance from the centre of the input gap to the centre of the output gap is L then the phase difference between the input and the output is

$$\phi = \omega L / u_0 \tag{39}$$

where the beam velocity is given by

$$u_0 = c\left[1 - \left(1 + (eV/m_0c^2)\right)^{-2}\right]^{0.5} \quad . \tag{40}$$

Thus if the normal beam voltage is 90 kV, the tube length 1.17 m, and the frequency 500 MHz, the sensitivity of phase to changes in the beam voltage is –5.8° per kV.

The transfer characteristic of a klystron with synchronously tuned cavities is essentially that of a resonant circuit as far as changes in frequency are concerned, namely

$$H(\omega) = R/\left[1 - jQ(\omega_0/\omega - \omega/\omega_0)\right] \quad . \tag{41}$$

The effective Q factor takes account of the combined effects of all the cavities and of any external loading. The klystron used in the example above has a bandwidth of 1 MHz, giving an effective Q factor of 500. Small changes in the centre frequency are produced by changes in the working temperature of the tube. If $\omega = \omega_0 + \delta\omega$ and if $\delta\omega$ is small then

$$\text{phase}(H(\omega)) = \arctan(-2Q\delta\omega/\omega_0) \quad , \tag{42}$$

giving a phase sensitivity of -63° per MHz. If the cavities are made from copper, whose coefficient of thermal expansion is 16×10^{-6} K^{-1}, then the sensitivity of phase to variations in temperature is 0.53 degrees/K.

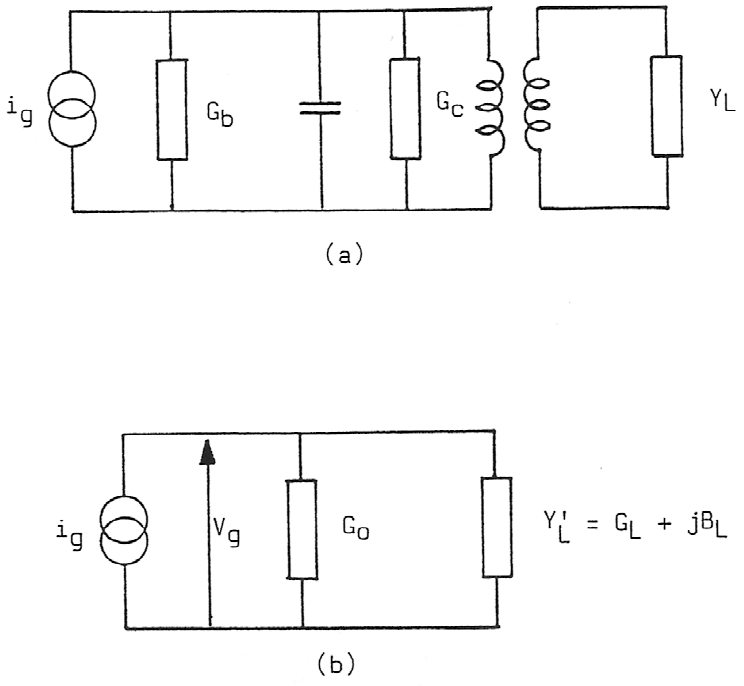

Fig. 23: Equivalent circuits of the output of a klystron

The output circuit of a klystron can be represented by the equivalent circuit shown in Fig. 23(a). The beam behaves as a current source with an impedance R_b, which is of the order of 20 kΩ. The shunt resistance of the output cavity, R_c, is in the range 50 to 200 kΩ. The transformer represents the output coupling and matching network required to match the load impedance Z_L to the output impedance of the klystron. Some klystrons incorporate arrangements for adjusting the coupling between the load and the cavity. If the cavity is tuned to the signal frequency the equivalent circuit can be simplified to that shown in Fig. 23(b). The load admittance is referred to the plane of the output gap as $Y'_L = G_L + jB_L$. When the load is correctly matched to the tube $G_L = R_b$ and $B_L = 0$. The effects of a mismatched load can be deduced from the circuit in Fig. 23(b). The gap voltage is given by

$$V_{\rm g} = i_{\rm g}/(G_0 + G_{\rm L} + jB_{\rm L}) \ . \tag{43}$$

When the load is matched

$$V_{\rm g} = V_{\rm g0} = i_{\rm g}/2G_0 \ . \tag{44}$$

Thus

$$V_{\rm g}/V_{\rm g0} = 2G_0/(G_0 + G_{\rm L} + jB_{\rm L}) = 2/(1 + g_{\rm L} + jb_{\rm L}) \ , \tag{45}$$

in which the lower case symbols represent admittances that have been normalized to that of a matched load. Then the normalized gap voltage has amplitude

$$|V_{\rm g}/V_{\rm g0}| = 2/\left[(1+g_{\rm L})^2 + b_{\rm L}^2\right]^{1/2} \tag{46}$$

and phase

$$\text{phase}\,(V_{\rm g}/V_{\rm g0}) = \arctan\left[-b_{\rm L}/(1+g_{\rm L})\right] \quad . \tag{47}$$

The power delivered to the load is

$$P_{\rm L} = 0.5\,|V_{\rm g}|^2\,G_{\rm L} \tag{48}$$

and to a matched load is

$$P_0 = 0.5\,|V_{g0}|^2\,G_0 \tag{49}$$

so that

$$P_{\rm L}/P_0 = 4\,g_{\rm L}/\left[(1+g_{\rm L})^2 + b_{\rm L}^2\right] \quad . \tag{50}$$

Contours of constant gap voltage amplitude and of constant load power can be calculated from Eqs. (44) and (48). Figure 24 shows these contours plotted on a Smith chart of normalized load admittance for a typical klystron [18]. It is important to ensure that the working point remains in the region for which the normalized gap voltage is less than unity in order to avoid the risk of voltage breakdown in the output gap. If the gap voltage becomes too high it is possible for electrons to be reflected, reducing the efficiency of the tube and providing a feedback path to the other cavities, which may cause the tube to become unstable. A further complication is provided by the effect of harmonic signals in the output cavity. Since the klystron is operated in the non-linear regime to obtain maximum efficiency it follows that the signal in the output waveguide will have harmonic components. These are incompletely understood but it is known that the reflection of harmonic signals from external components such as a circulator can cause the klystron output to behave in unexpected ways.

5.3 Typical klystrons

5.3.1 UHF television klystrons

At moderate powers in the UHF band it is possible to use klystrons designed for use in UHF television transmitters as power sources for accelerators. Tubes are available with output powers in the 10–70 kW range and gains of 30–40 dB. The beam current can usually be controlled independently of the beam voltage by the voltage applied to a separate modulating anode. The conversion efficiency is around 50% but in some modern tubes this is increased by the use of a multi-element depressed collector. This type of collector has several electrodes at different potentials between ground and cathode potentials. The spent electron beam can therefore be collected in a way that reduces both the heat dissipated in the collector and the power supplied to the tube [19]. If greater power is required than can be supplied by one tube it is possible to operate several tubes in parallel. A 450 kW, 800 MHz amplifier for the CERN SPS comprises eight modified UHF television klystrons operated in parallel.

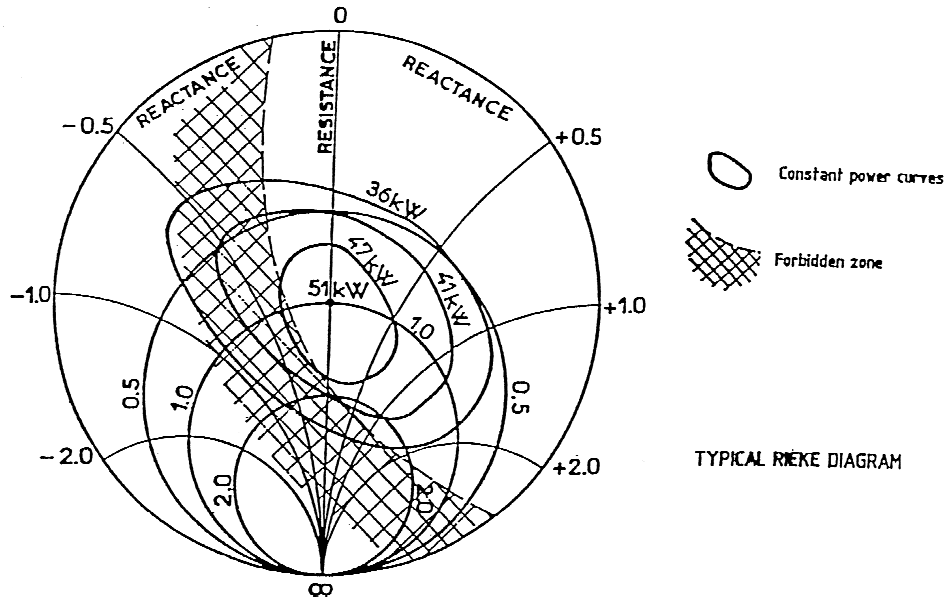

Fig. 24: Typical Rieke diagram of a klystron (courtesy of Thales)

5.3.2 Super-power klystrons

Some klystrons, commonly known as super-power klystrons, have been developed specifically for use in accelerators. Tables 5 and 6 give a summary of the characteristics of some typical tubes.

Table 5: Characteristics of typical CW super-power klystrons

Type	**TH2089B**	**K351C**	**YK1303**	**TH2103**	**Units**
Frequency	352	352	508	3700	MHz
Beam voltage	100	100	90	60	kV
Beam current	20	20	18.2	20	A
Power	1300	1300	1	0.5	kW
Efficiency	65	65	61	43	%
Gain	40	40	41	45	dB
Length	4.8	3.8	3.75	2.0	m

Table 6: Characteristics of typical pulsed super-power klystrons

Type	**TH 2153**	**SLAC**	**VKS 8333A**	**Units**
Frequency	3.0	2.87	2.998	GHz
Beam voltage	576	470		kV
Beam current	600	612		A
Power	150	150	150	MW
Pulse length	1.2	3	3	μsec
Efficiency	43	50		%
Gain	48	52		dB

5.4 The SLAC Energy Doubler

Sometimes higher pulsed powers are required than can be obtained from a single conventional klystron. One way of achieving this is the energy doubler devised at SLAC (SLED) [20]. The principle of operation of this device is illustrated by Fig. 25(a). The input to the klystron is via a 180° switched phase shifter. The output passes to a 3 dB coupler connected to a pair of cavities. If the cavity fields are initially zero then part of the output power of the klystron goes into building them up while the remainder is reflected and passes on towards the accelerator. As the cavity fields increase they re-radiate power in anti-phase with the incident signal so that the mean power transmitted to the accelerator is small. The cavities are over-coupled so that the peak re-radiated power rises to a level greater than the transmitted power. If the phase of the klystron drive is then abruptly reversed the re-radiated and transmitted signals are in phase with each other and the power transmitted to the accelerator rises steeply, as shown in Fig. 25(b). The power level then decays as the energy stored in the cavities is discharged. The process can be repeated to provide a train of very high energy pulses. The principle is similar to that of a pulse modulator with RF storage in the cavities replacing d.c. storage in capacitors. The original SLED system [20] used a pulsed 30 MW klystron to produce SLED output pulses at 125 MW. More recently a similar system has been suggested that employs a CW klystron [21].

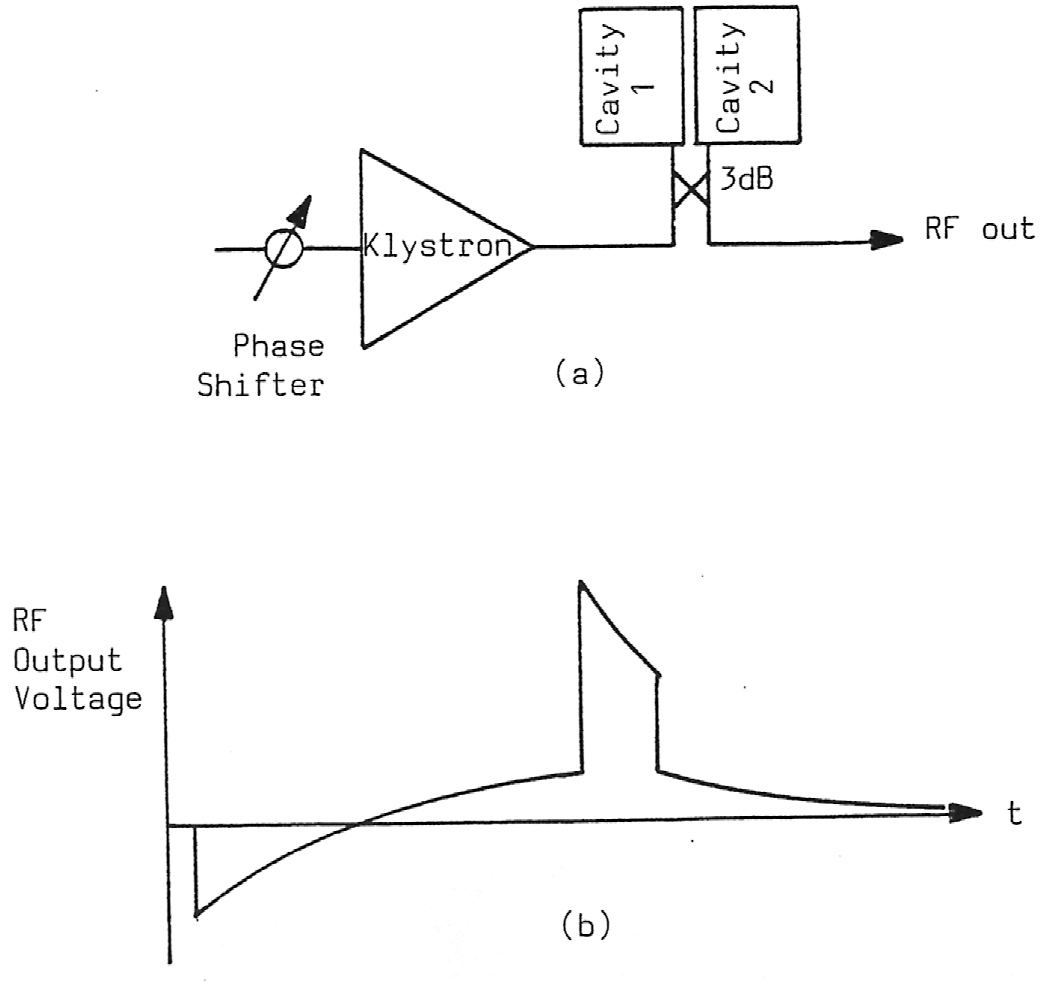

Fig. 25: The SLAC Energy Doubler (SLED): (a) circuit diagram and (b) output waveform

5.5 Multiple beam klystrons

We have seen that the efficiency of a klystron is determined by the perveance of the electron beam, so, to get high efficiency, it is necessary to use a high-voltage, low-current beam. The use of high voltages produces problems with voltage breakdown and it is therefore difficult to obtain very high power with high efficiency, as can be seen by comparing Table 6 with Table 5. One solution to this problem is to use several electron beams within the same vacuum envelope, as shown in Fig. 26. A klystron designed in this way is known as a Multiple Beam Klystron (MBK). The principle of the MBK has been known for many years [22] but, until recently, the only such tubes constructed were in the former Soviet Union, for military applications. The first MBK designed specifically for use in particle accelerators is the TTE type TH1801, whose performance is shown in Table 7 [23].

Table 7: Characteristics of a multiple beam klystron

Type	**TH 1801**	**Units**
Frequency	1300	MHz
Beam voltage	115	kV
Beam current	133	A
Number of beams	7	
Power	9.8	MW
Pulse length	1500	μs
Efficiency	64	%
Gain	47	dB

5.6 Relativistic klystrons

Some experimental work has been carried out on klystrons with very high energy beams produced by induction linear accelerators [24]. Table 8 shows the results achieved in one such experiment.

Table 8: Characteristics of the LLNL SL-4 relativistic klystron

Type	**TH 1801**	**Units**
Frequency	11.45	GHz
Beam voltage	975	kV
Beam current	625	A
Power	200	MW pk
Pulse length		μs
Efficiency	32	%
Gain	55	dB

6 GYROTRONS

An alternative type of tube for producing very high pulsed RF power at high frequencies is the gyrotron. This type of tube has been the subject of intensive developmental work mainly with a view to providing RF power for plasma heating experiments. A good summary of this work and of the development of other, novel, high-power RF sources is given in Ref. [25]. The gyrotron employs the interaction between an annular electron beam and the azimuthal electric field of a circular waveguide mode, as shown in Fig. 27. There is a strong axial magnetic field so that the electrons move in small orbits at the cyclotron frequency within the beam (as shown). The cyclotron frequency is made equal to the signal frequency.

At frequencies above 60 GHz this means that a super-conducting solenoid is needed to produce the magnetic field. It is essential to the working of the gyrotron that the electrons should have relativistic velocities. The cyclotron frequency is then given by

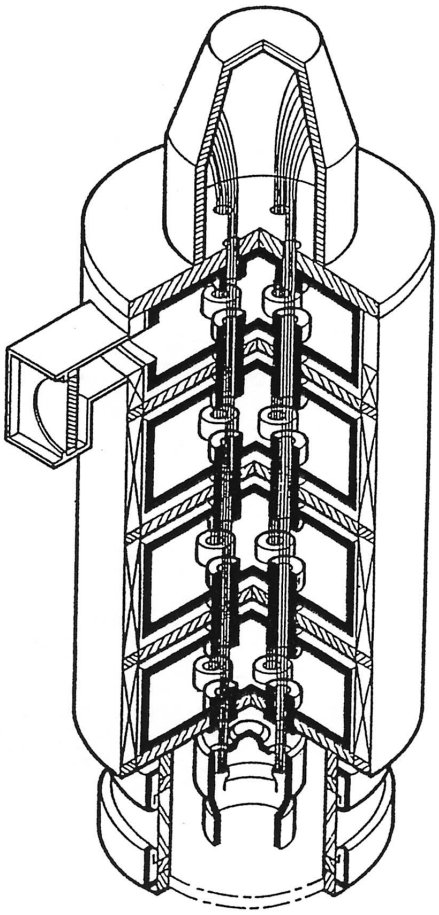

Fig. 26: Schematic diagram of a multiple-beam klystron (MBK) (courtesy of Thales)

$$\omega_c = (eB/m_0)(1 - \nu^2/c^2)^{0.5} \tag{51}$$

so that it is a function of the electron velocity. As the electron velocity increases the cyclotron frequency decreases so that the faster electrons lag behind the field. Slow electrons, similarly, lead the RF field and phase bunching occurs with a net transfer of energy to the RF field.

Commercially available gyrotrons are oscillators with the general arrangement shown in Fig. 28. The hollow electron beam is produced by a magnetron electron gun and confined by an axial magnetic field whose strength varies as shown. The interaction takes place in a section of cylindrical waveguide made resonant by the mismatches at its ends. The spent electron beam is allowed to spread sideways to be collected on the wall of the larger, cylindrical, output waveguide. The RF output power passes down this guide and through the output window. At millimetre wavelengths it is usual to use an over-moded output waveguide to avoid problems with breakdown in it. Table 9 shows the characteristics of some typical gyrotron oscillators.

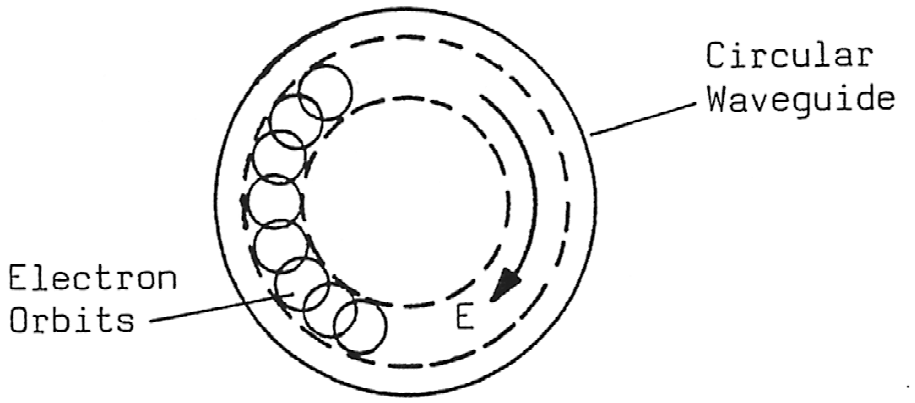

Fig. 27: Principle of operation of a gyrotron

Table 9: Characteristics of typical pulsed gyrotron oscillators

Type	**TH1504**	**TH1503B**	**Units**
Frequency	8	110	GHz
Beam Voltage	90	80	kV
Beam Current	27	15	A
Power	1	0.35	MW
Efficiency	41	29	%

Experimental gyrotron amplifiers have been made that are analogues of klystrons and travelling-wave tubes. These tubes are potentially better than klystrons for producing multi-megawatt RF pulses at frequencies of 20 GHz and above.

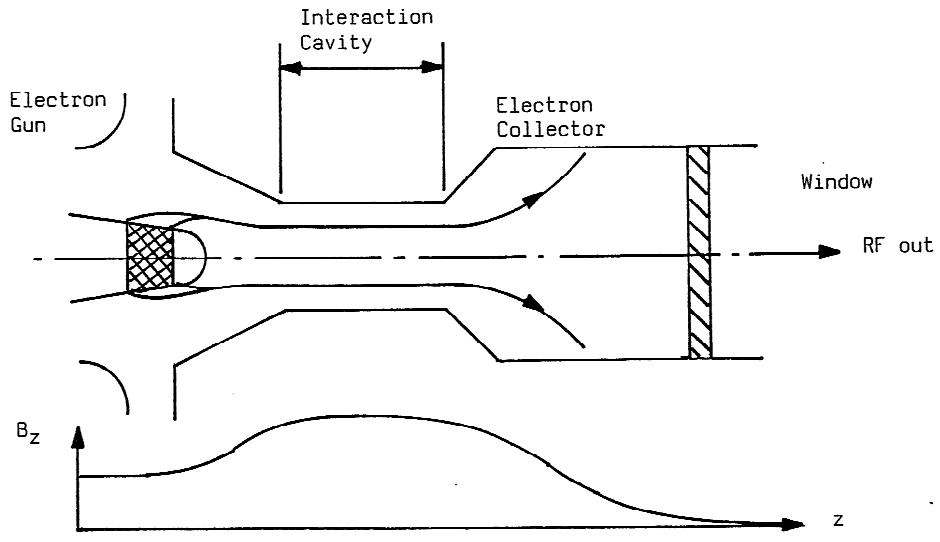

Fig. 28: Arrangement of a gyrotron oscillator

7 LIMITATIONS OF MICROWAVE TUBES

The performance of microwave tubes is limited by a number of factors, which operate in much the same way for both klystrons and gyrotrons. The chief of these are heat dissipation, voltage breakdown, output window failure, and multipactor discharges.

The RF structures and the windows of microwave tubes generally scale inversely with frequency. The maximum CW or average power that can be handled by a particular type of tube depends upon the maximum temperature that the internal surfaces can be allowed to reach. Now this temperature is independent of the frequency, so the power that can be dissipated varies inversely with the frequency. Gyrotrons can handle a higher power of the same frequency than klystrons because they have simpler structures and, if operated in a higher order mode, their structures are larger for a given frequency.

The power is also limited by the power that can be generated by an electron gun and formed into a beam. The beam diameter scales inversely with frequency and the beam current density is determined by the maximum attainable magnetic focusing field. Since the field is independent of frequency the beam current scales inversely with the square of the frequency. The beam voltage is related to the current by the gun perveance ($I/V^{1.5}$), which usually lies in the range 1.0 to 2.0 for power tubes. The maximum gun voltage is limited by the breakdown field in the gun and so varies inversely with frequency for constant perveance. These considerations suggest that the maximum power obtainable from a tube of a particular type varies as frequency to the power –2.5 to –3.0, depending upon the assumptions made. For pulsed tubes the peak power is limited by the considerations mentioned here and the mean power by those mentioned above. The efficiencies of tubes tend to fall with increasing frequency. This is partly because the RF losses increase with frequency and partly because of the design compromises that must be made at higher frequencies.

The maximum power obtainable from a pulsed tube is often determined by the power-handling capability of the output window. The output window of an external cavity klystron is in the form of a cylinder within the cavity and close to the output gap. This arrangement is limited to powers of about 70 kW. At higher power levels integral cavities are used and the power is brought out through waveguide or coaxial line windows. Very high power klystrons commonly have two windows in parallel to handle the full output power. Windows can be destroyed by excessive reflected power, by arcs in the output waveguide, by X-ray bombardment, and by the multipactor discharges described in the next Section. The basic cause of failure is overheating and it is usual to monitor the window temperature and to provide reverse power and waveguide and cavity arc detectors.

7.1 Multipactor discharge

Radio frequency vacuum breakdown can happen in a variety of ways, all described as multipactor discharges. The basic mechanism is illustrated by Fig. 29, which shows a pair of parallel metal plates in vacuum with a sinusoidally varying voltage between them. If an electron is liberated from one of the plates at a suitable phase of the RF field it will be accelerated towards the other plate and may strike it and cause secondary electron emission. If the phase of the field at the moment of impact is just 180° from that at the time when the electron left the first plate, then the secondary electrons will be accelerated back towards the first plate. These conditions make it possible for a stable discharge to be set up if the secondary electron emission coefficients of the surfaces are greater than unity. It is found that electrons liberated at a phase of the RF field lying within a certain range of the ideal one tend to reach the other electrode at a phase closer to the ideal.

The secondary emission coefficients of many materials vary with the energy of electrons with normal incidence according to the universal curve shown in Fig. 30. The constants of this curve for a number of materials used in vacuum tubes are given in Table 10.

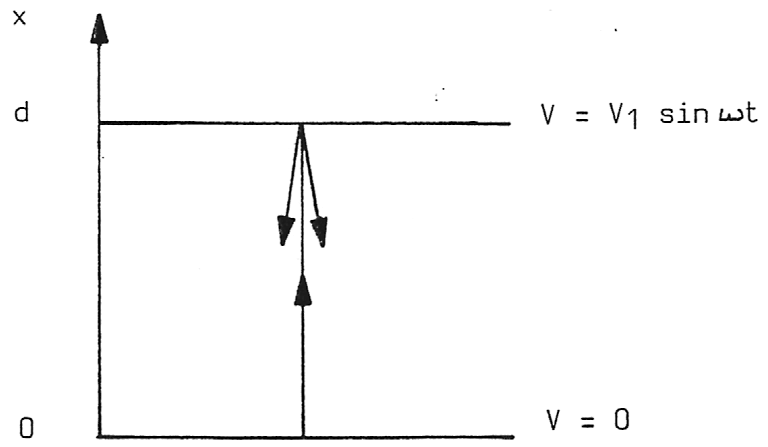

Fig. 29: Principle of the multipactor discharge

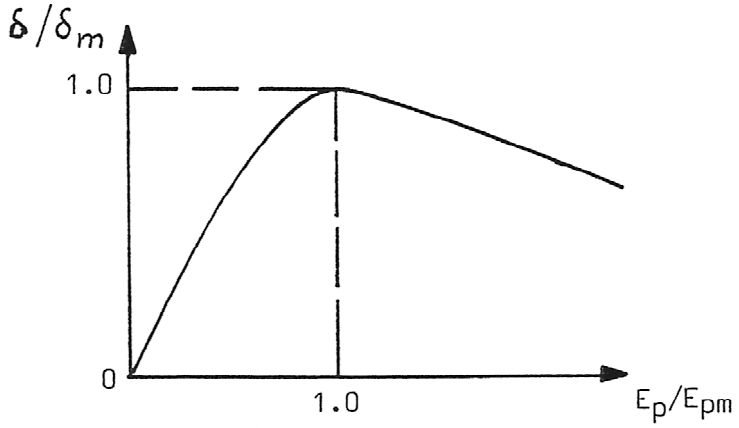

Fig. 30: Variation of secondary electron emission coefficient with primary electron energy

Table 10: Secondary electron emission coefficients of materials used in vacuum tubes

Material	δ_m	E_{pm} **(V)**
Copper	1.3	600
Platinum	1.8	800
Carbon	0.45	500
Alumina	2.35	500

A two-surface multipactor discharge can, therefore, only occur within a fairly limited range of voltages and products of frequency and electrode separation, as illustrated by Fig. 31. The limits in the vertical direction are set by the need for the secondary electron emission coefficient to be greater than unity. Table 10 shows that this happens for a small range of energies of the order of a few hundred electron volts. The limits in the horizontal direction are set by the need for the correct phase relationships. Figure 31 also shows the ranges in which higher order multipactor discharges can occur. The two-surface multipactor discharge typically involves currents of less than 1 A and voltages of a few hundred volts, so the power is moderate and the discharge is not normally destructive. It is probable that discharges of

this kind occur in most microwave power tubes and their main effect is to cause some additional loss and loading of the RF circuit.

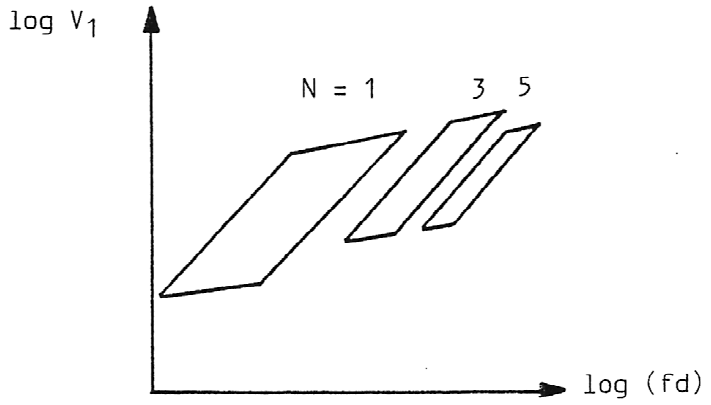

Fig. 31: Ranges in which two-surface multipactor discharges can occur

A more serious kind of multipactor discharge can occur in the presence of a magnetic field, as shown in Fig. 32. The electron trajectories are bent by the field so that the impacts made on the surfaces are oblique. This type of discharge can involve impacts on either one or two surfaces. Figure 33 shows the effects of oblique incidence on the secondary electron emission coefficient of a surface. First the peak value of δ is greater for oblique incidence than for normal incidence, and second, the range of energies over which δ is greater than unity is greatly increased. Thus crossed-field multipactor discharges can occur at much higher energies than the simple multipactor and they are, in consequence, potentially much more damaging. Because strong magnetic fields are used to focus linear-beam tubes it is quite possible for the conditions for crossed-field multipactor to exist somewhere within the tube. The manufacturer will normally have taken steps to ensure that this is not the case but, if the magnetic field around the tube is disturbed in any way (by the field of a circulator for example), then it is possible for a destructive discharge to occur.

It is also possible for multipactor discharges to occur on ceramic surfaces, with surface charge providing a static field. The local heating of a window ceramic in this way can be sufficient to cause window failure. Further information about multipactor discharges can be found in Ref. [26].

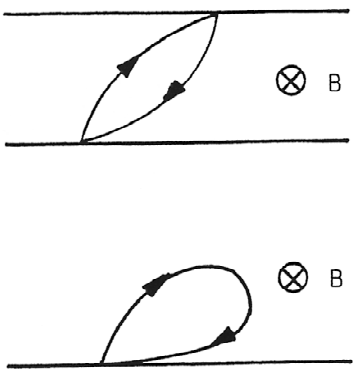

Fig. 32: Crossed-field multipactor discharges

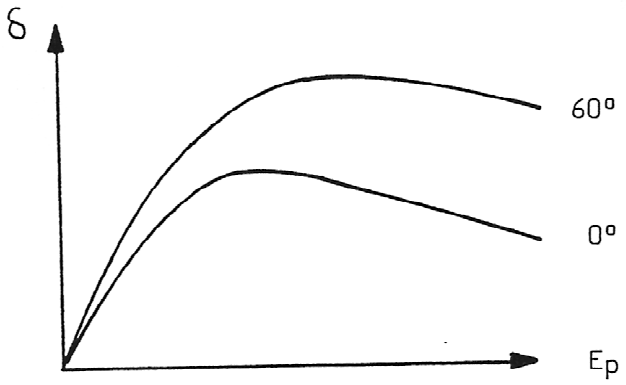

Fig. 33: Effect of the angle of incidence on secondary electron emission coefficient

8 COOLING AND PROTECTION

8.1 Cooling power tubes

The power tubes used in accelerators typically have efficiencies between 40% and 70%. It follows that a proportion of the d.c. input power is dissipated as heat within the tube. The heat to be dissipated is between 40% and 150% of the RF output power provided that the tube is never operated without RF drive. If a linear beam tube is operated without RF drive then the electron collector must be capable of dissipating the full d.c. beam power. The greater part of the heat is dissipated in the anode of a tetrode or in the collector of a linear-beam tube. These electrodes are normally cooled in one of three ways: by blown air (at low power levels); by pumped liquid (usually de-ionized water); or by vapour phase cooling. The last of these may be less familiar than the others and needs a little explanation.

The electrode to be cooled by vapour phase cooling is immersed in a bath of the liquid (normally de-ionized water), which is permitted to boil. The vapour produced is condensed in a heat exchanger, either in the cooling tank or part of an external circuit. The cooling system therefore forms a closed loop so that water purity is maintained. In all water cooling systems it is important to maintain the water purity to ensure that the electrodes cooled are neither contaminated nor corroded. Either of these effects can degrade the effectiveness of the cooling system and cause premature failure of the tube. In blown air systems careful filtering of the air is necessary for the same reasons.

It is important to remember that, in a high power tube, appreciable quantities of heat will be dissipated on parts of the tube other than the anode or collector, especially if a fault occurs during operation. It is common to provide air or water cooling for these regions too. Inadequate cooling may lead to the internal distortion or melting of the tube and its consequent destruction. Further information on the cooling of tubes is given in Refs. [7, 8].

8.2 Tube protection

Power tubes are very expensive devices and it is vital that they are properly protected when in use. The energy densities in the tubes and their power supplies are so high that it is easy for a tube to be destroyed if it is not properly protected. However, with adequate protection tubes are in fact very good at withstanding accidental overloads and may be expected to give long, reliable service.

Two kinds of protection are required. First, a series of interlocks must be provided to ensure that the tube is switched on in the correct sequence. It must be impossible to apply the anode voltage until the heater is at the correct working temperature, the cooling systems are functioning correctly, and

so forth. The exact switch-on sequence depends upon the tube type and reference must be made to the manufacturer's operating instructions. The sequence must also be maintained if the tube has to be restarted after tripping off for any reason.

The second provision is of a series of trips to ensure that power is removed from the tube in the event of a fault such as voltage breakdown, excessive reflected power, and so forth. Again, the range of parameters to be monitored and the speed with which action must be taken varies from tube to tube. Examples are coolant flow rate, coolant temperature, tube vacuum, output waveguide reverse power, and electrode over-currents. If a tube has not been used for some time it is sometimes necessary to bring it up to full power gradually to avoid repeated trips. The manufacturer's operating instructions should be consulted. If a tube trips out repeatedly it is wise to consult the manufacturer to avoid the risk of losing the tube completely by unwise action taken in ignorance of possible causes of the trouble. General information about tube protection and safe operation is given in Refs. [7, 8].

9 CONCLUSION

This paper has set out to review the main types of RF power source used in particle accelerators. In conclusion we review the state of the art of the different types of power source.

Figure 34 shows the state of the art for RF power sources in terms of their CW or mean powers as a function of frequency. Solid-state sources can only compete with tubes at the lower frequencies and power levels and even that requires massively parallel operation, as noted in Section 2. The fall-off in power output at high frequencies for each type of tube is related to the fundamental principles of its operation, as discussed in Section 7. The power achieved by klystrons at low frequencies does not generally represent a fundamental limitation but merely the maximum that has been demanded to date. For tetrodes and solid-state devices the maximum power is probably closer to the theoretical limits for those devices. In any case higher powers can be produced by parallel operation.

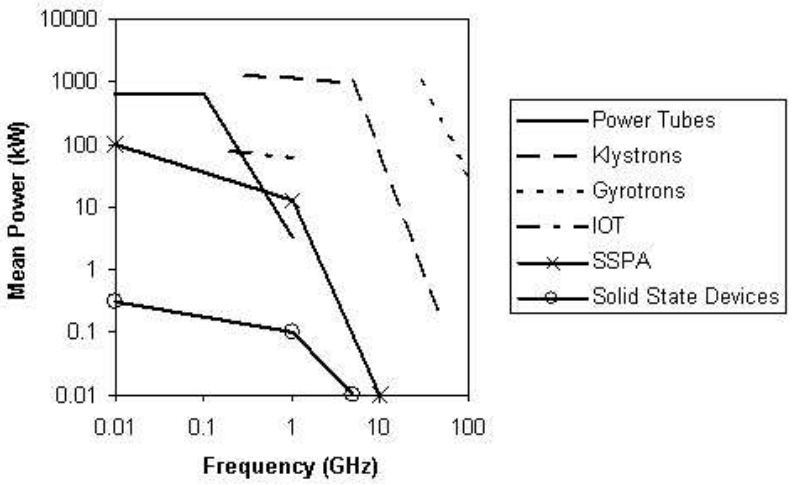

Fig. 34: Output power of state of the art of continuous wave sources

Figure 35 shows the state of the art of the devices discussed in terms of their efficiencies as a function of frequency. In general the efficiency of any kind of device falls with increasing frequency for the reasons discussed in Section 7. The overall efficiencies of linear-beam tubes designed for the lower power levels can be increased by collector depression. Super-power tubes do not have separately insulated collectors.

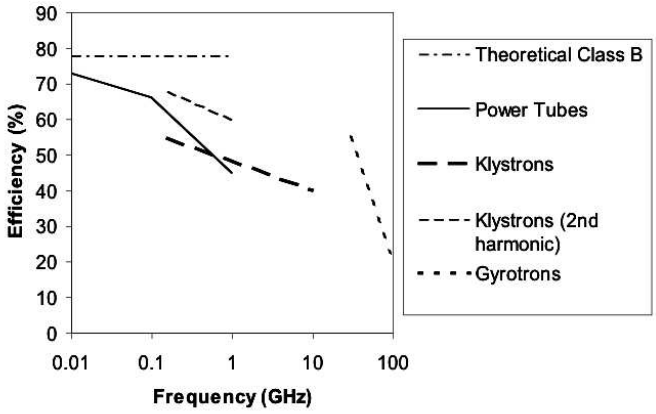

Fig. 35: Efficiencies of state-of-the-art continuous wave sources

Finally, Fig. 36 shows the state of the art for pulsed RF power sources. The figure includes conventional microwave tubes, relativistic derivatives of conventional tubes and gyrotrons. It also shows a number of other experimental devices which have not been discussed in this paper. Further information is given in Ref. [25].

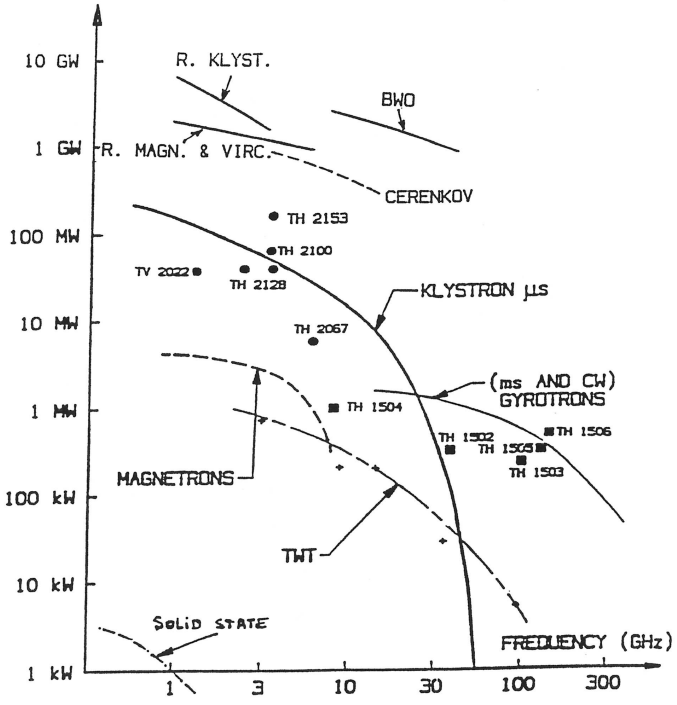

Fig. 36: Peak output power of state-of-the-art pulsed sources (Courtesy of Thales)

For further information on the theory of microwave tubes and for suggestions for background reading see Refs. [27–29].

ACKNOWLEDGEMENTS

This paper could not have been written without the generous help of a number of people. Special thanks are due to D. Carr and R. Heppinstall of Marconi Applied Technologies, H. Bohlen of CPI, H.P. Kindermann and H. Frischholz of CERN, V.P. Suller and his colleagues at the SERC Daresbury Laboratory, J. Stahl of Siemens, J. Vogel of Philips, F. Bernier and G. Faillon of Thomson Tubes Electroniques, and R.A. Rimmer of the Lawrence Berkeley Laboratory.

REFERENCES

[1] C. Zettler, RF systems for accelerators, CERN 87–10 (1987).

[2] C. Davis, J. Hawkins, and C. Einholf Jr., *IEEE Trans. Broadcasting*, **43** (1997) 252.

[3] T. Ikegami, A newly design UHF solid-state television transmitter, IEE Colloquium Digest No. 1988/16 (1988).

[4] CY1172 RF Power Tetrode data sheet, EEV Ltd., 1990.

[5] K. Spangenburg, *Vacuum Tubes*, McGraw-Hill (1948).

[6] W. Herdrich and H.P. Kindermann, RF power amplifier for the CERN SPS operating as LEP injector, Proc. Particle Accelerator Conf., Vancouver, 1985.

[7] Transmitting Tubes Data Book 1986/87, Siemens AG, 1986.

[8] Preamble–Tetrodes, EEV Ltd., 1976.

[9] T. Fujisawa et al., *Nuclear Inst. Methods Phys.Res.* **A292** (1990) 1.

[10] G. Schaffer, Components for high-power RF systems in modern accelerators, Lecture given at the 3rd Workshop New Techniques for Future Accelerators, Erice-Trapani, May 1987.

[11] W. Herdrich, H.P. Kindermann, and W. Sinclair, The RF power plant of the SPS, Proc. Particle Accelerator Conf., Santa Fe, 1983.

[12] A. Boussaton, G. Clerc, J.P. Ichac, and C. Robert, A new generation of gridded tubes for c.w. operation on new fusion magnetic machines, 1997 Symposium on Fusion Engineering, San Diego, California, October 6–10, 1997.

[13] G. Clerc, *Diacrode ®: Fundamentals and Performance*, Thomson Tubes Electroniques (1997).

[14] D.H. Preist and M.B. Shrader, The klystrode–an unusual transmitting tube with potential for UHF TV, Proc. IEEE, **70** (1982) 1318.

[15] H. Bohlen, Advanced high power microwave vacuum electron device development, Proc. 1999 Particle Accelerator Conference, New York, p. 445.

[16] H. Bohlen, CPI Inc., Private communication.

[17] G. Faillon, Technical and industrial overview of RF and microwave tubes for fusion, *Fusion Engineering and Design*, **46** (1999) 371.

[18] G. Faillon, Klystrons and related devices, Presented at the 48th Scottish Universities Summer School in Physics: Generation and Application of High Power Microwaves, St. Andrews, 1996.

[19] H. Bohlen *et al.*, Improved technological solutions for UHF power tubes, EEV Ltd., 1990.

[20] Z.D. Farkas *et al., IEEE Trans. Nucl. Sci.*, **NS-22** (1975) 1299.

[21] Z.D. Farkas, RF energy compressor, IEEE MTT Society, Int. Microwave Symposium Digest, 1980, p. 84.

[22] M.R. Boyd, R.A. Dehn, J.S. Hickey, and T.G. Mihran, *IRE Trans. Electron Devices*, **ED-9** (1962) 247.

[23] A. Beunas and G. Faillon, 10 MW/1.5ms, L-band multi-beam klystron, Proc. Conf. Displays and Vacuum Electronics, Garmisch-Partenkirchen, Germany, 1998, p. 257.

[24] Allen, RF power sources, Proc. 1988 European Particle Accelerator Conf., Rome, 1988, p. 101.

[25] V.L. Granatstein and I. Alexeff (eds.), *High-Power Microwave Sources*, Artech House (1987).

[26] J.R.M. Vaughan, *IEEE Trans. Electron Devices*, **ED-35** (1988) 1172.

[27] M.J. Smith and G. Phillips, *Power Klystrons Today*, Research Studies Press (1995).

[28] A.S. Gilmour, *Microwave Tubes*, Artech House (1986).

[29] L. Sivan, *Microwave Tube Transmitters*, Chapman and Hall (1994).